Analysis of Single-Diode and Improvement of Double-diode Photovoltaic Source Modelling Methods and Techniques

Samkeliso Hubert Shongwe

August 2015

Dissertation submitted for the degree of
Master of Science in Electrical Engineering

Faculty of Engineering and the Built Environment
Department of Electrical Engineering
University of Cape Town

Abstract

Modelling of photovoltaic systems is essential for designers of solar generation plants to do a yield analysis that accurately predicts the expected power output under changing environmental conditions. There are a few different models which are used and they all differ in their implementation and also on the accuracy.

The main aim of this thesis is to analyse different PV modelling methods which are based on the single-diode and double-diode models. The study carried out, falls under two sections. The first study was to figure out which single-diode model produces the most accurate results. The second study is extended to double-diode models. Here, the thesis goes on to propose a different PV modelling method which is based on the double-diode representation of a PV module that will be verified and compared with other models and experimental data.

An analysis of the various different single-diode models is done based on two commercially available PV modules: SQ80 and the KC200GT, in which the simulated results are compared with the characteristics extracted from the datasheets. Parameter estimation techniques within a modelling method are generally used to estimate the five unknown parameters in the single-diode model. Two sets of estimated parameters were used to plot the I-V characteristics of two PV modules, SQ80 and KC200GT, for the different sets of modelling equations which are classified into models 1 to 5 in this study. Each model is based on the different combinations of diode saturation current and photo generated current, plotted under varying irradiance and temperature. Modelling was done using Matlab/Simulink software and the results from each model were first verified for correctness against the results produced by their respective authors, then a comparison was made amongst the different models (models 1 to 5) with respect to experimentally measured and datasheet I-V curves. The SQ80 module is also connected in the lab and experimental values are measured from it under different environmental conditions. A comparison is then made using the different modelling methods with the experimental data to evaluate the accuracy of the models.

In the second study, the new proposed double-diode PV modelling method is also implemented using datasheet information for three commercial PV modules made from different technologies: mono-crystalline, poly-crystalline and thin-film

technology. This method is an improvement on an existing method and is more accurate. A comparison is made with the characteristics extracted from the datasheet to verify that it produces accurate results. A comparison of this modelling method is also made with the experimentally measured data from the SQ80 PV module.

The results obtained were used to draw conclusions on which combination of parameter extraction and modelling method best emulates the manufacturer's characteristics.

Declaration

I know the meaning of plagiarism and declare that all the work in the document, save for that which is properly acknowledged, is my own.

I certify that this dissertation reports original work by me during my University research and each quotation from other people's work used in this report has been cited and listed under references.

Signature…. Signed by candidate …. **Date**…16 – 11 – 2015……..

Acknowledgements

Firstly I would like to thank my manager Mr. Vusi Anderson Gama at Swaziland Electricity Company for seconding and facilitating the funding for me to be able to attend full time study for a Master's degree.

I would also like thank my supervisor Dr. Moin Hanif who guided me through the research. I would like to thank him for the direction, assistance, and encouragement he provided to ensure that this research is completed. I am honoured to have worked with him.

Thank you also to the machines laboratory principal technical officer Mr. Chris Wozniak for his assistance in setting up the data collection equipment.

I am also grateful to my family, friends and also to my colleagues in the Power Electronics Research Group for moral support during my time at the University, it would not be the same without them. To my wife Nomfundo who had to endure hardships at home while I was away at school, I am very grateful.

Above all, I would like to thank the almighty God for providing strength to endure the tough times during the course of the research.

Table of Contents

List of Figures

List of Tables

1 Introduction

1.1 Background and Context

In the face of global climate change, increasing the use of renewable energy resources is one of the most urgent challenges facing the world as it is required that new sources of clean energy are utilized [1].

Solar power stations rely on the energy from the sun which is readily available to produce electricity using Photovoltaic (PV) panels [2]. It is one of the few abundantly available options as the world turns to renewable energy sources as a means to produce clean energy.

The use of solar energy to generate electricity is the most readily accessible resource in South Africa and the rest of Africa, with most areas averaging more than 2 500 hours of sunshine per year, and average solar-radiation levels ranging between 4.5 and 6.5kWh/m^2 in one day. It lends itself to a number of potential uses and the country's solar equipment industry is developing. Annual photovoltaic (PV) panel assembly capacity totals 5MW, and a number of companies in South Africa manufacture solar water heaters [3]. This shows the high potential of growth in the solar power generation industry in the Southern African region.

In addition, the energy shortage in most African countries, especially South Africa has prompted the implementation of several initiatives such as the Renewable Energy Independent Power Producer Procurement Program which increases the interest from investors in renewable energy projects. Such projects have a potential of bringing R100-billion worth of foreign and local investment [4].

An article in [5] reveals that by 2030, renewable energy would contribute 42% of the South African power demand, because it is becoming increasingly competitive with ESKOM tariffs which uses mainly fossil fuel for electricity generation. The article also mentions that there has been a reduction in solar tariffs over three successive bidding rounds of Renewable Energy Independent Power Producer Procurement Program (EIRPPPP) from R3/kWh to R1/kWh, showing the great potential of growth in solar power generation.

This growth in solar energy production also presents areas of research which require a lot of consideration. Under consideration is the prediction of PV energy production (modelling) coupled with optimal choice and design of power converters interfacing the

PV generators to the utility load [6]. The main aim of an accurate mathematical model of a PV module or cell is to optimize the design and dimensioning of PV power plants to maximize their power generation capability [7] and also to be able to accurately define specifications for the power conditioning equipment. Modelling involves mathematically expressing the behavior of PV module current and power with respect to voltage under varying conditions of temperature and irradiance. It requires two steps; the first step is parameter estimation where a specific technique is applied to predict or estimate the unknown parameters required to complete a model and the second step is to use these estimated parameters within the modelling equations that produce the graphs depicting the behaviour of the modules under varying temperature and irradiance. In the single-diode model there are 5 unknown parameters to be estimated and for the double-diode model there are 7 unknown parameters.

The information available to develop the model of a PV module is obtained from the manufacturer's datasheet, which is readily available. It is common practice that the information provided in the manufacture's datasheet be specified under standard test conditions (STC), where the irradiance is 1kW/m^2 and the module temperature is 25 ºC (298K). Parameters typically provided by the manufacturers under STC are the maximum power (P_{mp}), short circuit current (I_{sc}), open circuit voltage (V_{oc}), current at maximum power point (I_{mp}), voltage at the maximum power point (V_{mp}), the number of series connected cells in a module (N_s) and temperature coefficients of temperature for short circuit current and open circuit voltage, i.e. K_I and K_V, respectively.

1.2 Scope and Objectives

The aim of the research is to identify different modelling methods based on the single-diode model and comparing them based on the parameter estimation method and the modelling equations in order to identify the most accurate combination of parameter estimation method and modelling equations.

It also aims to propose a new modelling method based on the double-diode model which will be tested, verified and compared for accuracy with other double-diode models currently presented in literature. This is an improvement on an already existing modelling method based on the double-diode model presented in [8].

The following was done in order to achieve the above stated objectives:

- A review of literature which deals with Photovoltaic source modelling using the single-diode model, the double-diode model, and also maximum power point tracking.
- A review of matlab simulation software and programing especially simulink to appreciate how it is used in modelling of photovoltaic cells and modules.
- Simulate different models based on the single-diode model and plot the characteristic I-V curves for comparison, using datasheet parameters for different modules as input.
- Analyse the behaviour of the double-diode model parameters with respect to changing unknown parameters and propose a model based on the double-diode model and perform simulations of different modules based on datasheet parameters as input.
- Carry out an experiment to measure the data from an actual photovoltaic module, which will be used to plot the characteristics of the PV module and also to verify the simulation results.
- Use the simulated plots as well as the experimentally measured data to do a comparison during analysis of the single-diode models as well as verification of the double-diode model.

1.3 Achievements and Research contribution

I have been able to carry out a detailed simulation study on single-diode models and compare the results to experimentally measured data. Based on the detailed comparison, the most accurate single-diode model is suggested.

I have also proposed, implemented and tested the double-diode model which describes analytical method of finding parameters for the double-diode model. This model is based on the simplified double-diode representation of a PV module.

1.4 Overview of Dissertation

In chapter 2 of this dissertation, a review of all the literature is presented, where all content which was consulted during this research will be briefly summarized to give and account of the previous research work in PV modelling.

Chapter 3 will give an outline of the single-diode model and will discuss the different modelling methods for the single-diode model with the purpose of comparing the different methods to find the most accurate method based on the combination of parameter estimating method as well as modelling equations. The different modelling methods are also validated with experimentally measured values from a commercial PV module.

Chapter 4 will introduce the new modelling method being proposed in this research and describe in detail how it is achieved. It is also verified by comparison with other methods as well as experimentally measured data.

In Chapter 5 the conclusions and evaluation of the research will be outlined.

2 Literature Review

The introduction of this dissertation briefly outlines background information on the advancements in the field of solar power generation and also mentions the need for accurate prediction of the yield of a PV generation plant. PV modelling is the mathematical presentation of a relationship between the current and voltage at the output terminals of a PV module and the main aim of an accurate mathematical model of a PV module or cell is to optimize the design and dimensioning of PV power plants to maximize their power generation capability [7] and also to be able to accurately define specifications for the power conditioning equipment.

A PV module consists of solar cells which are interconnected either in series or parallel or in some cases both. PV modules can be interconnected to form an array depending on the power requirements of the designer. A PV cell is represented by a circuit consisting of a current source connected in parallel to one diode, for single-diode representation and two diodes in parallel for the double-diode representation. A full model also includes a resistor connected in series to cater for external connections to the cell and another resistor connected in parallel (shunt resistor) to cater for the small leakage current which flows through the diode [9]. In the mathematical representation of the diode current equation for the full model, there exists 5 unknown parameters on the single-diode model and 7 unknown parameters for the double-diode model. Modelling requires that the parameters from the datasheet be used to estimate as accurately as possible these unknown parameters in order to complete the first step of modelling. The second step involves presenting a relationship between the current and voltage of the PV module under conditions other than STC.

Research work has already been carried out in order to come up with the most accurate model of a PV modules which uses the parameters obtained from the PV module manufacturer's datasheet and it all includes both the single-diode and double-diode versions. It has been stated that the double-diode representation of a PV module is more accurate than the single-diode model since the double-diode model describes the physical behaviour of a crystalline silicon cell at either high or low irradiance conditions [7] and also because it takes into account recombination losses [8], however the single-diode model is mostly preferred due to a combination of low complexity as well as accuracy.

On the single-diode model, authors in [10] presented another characteristic which

expresses voltage with respect to current by using the Lambert W function. This required that some or part of the expressions be neglected to simplify the computation and this affects the accuracy of the end result. It also introduces complexity as it requires the evaluation of the Lambert W function. Another approach employed in both single-diode and double-diode modelling is to develop models by using experimental data [2] and [11]-[18]. An experiment is set up using a specific module to measure the output voltage and current under different conditions to produce the characteristic plot which is then used to evaluate all parameters required for the model. [19] used a curve fitting technique to find the parameters for modeling. Even though a more practical result is obtained, this kind of approach however has the limitation of producing a model which is specific to that module, whereas a more general modeling technique is required which can be applicable to any module with the given datasheet parameters.

A better approach is to formulate equations or expressions for all the unknown parameters based on different modes of operation of the PV modules namely, open circuit operation, short circuit operation and maximum power point operation, [20]-[24]. However, this poses a challenge since these equations are nonlinear and transcendental in nature, therefore, it is difficult to find explicit solutions for them [25]. A number of iteration methods, termed numerical methods [26] have been proposed to find solutions to these equations. [20] uses Gaussian Iteration method, while [27] uses Newton Raphson method to solve the system of equations and [23] and [28] use particle swarm optimization.

Another approach, classified as an analytical method in [26], estimates one of the parameters to simplify the computation, but this may pose inaccuracies if the estimation is not accurate. Authors in [29] assumed a value of ideality factor and evaluated the other parameters, and [20] and [21] make the assumption that $I_{ph} = I_{sc}$ leaving only four parameters unknown. Also, authors in [21] defined a way to estimate the shunt resistance which is then used to evaluate the other four parameters from the equations. This however requires that the estimation be as accurate as possible otherwise large inaccuracies in these values can be obtained resulting in values which are far from the expected ones.

Another approach to find the parameters for the single-diode model is to use the equations but instead of estimation, one of the parameters is adjusted such that the corresponding values of current obtained matches a specific known condition such as

the maximum power point where the current and voltage are always known from datasheets. [15] and [29]-[31] choose values of series resistance starting from zero and incrementing the resistance until a specified and acceptable margin of error exists between the calculated value and the maximum power point values. [32] on the other hand uses the same technique but uses variation of the ideality factor based on the fact that its value ranges from 1 to 2.

All the above work presents different combinations of parameter estimation method and modeling equations used for finding the relationship between the PV current and PV voltage for a particular module using datasheet parameters under varying irradiance and temperature conditions. The aim of this research study is to find a combination of parameter estimation method and modelling equations which will provide the most accurate results from the previously proposed methods on the single-diode model.

The double-diode model has been investigated as well in the second part of this research study. The double-diode representation presents the complexity of extracting 7 unknown parameters in the double exponential expression of the diode current versus the 5 unknown parameters for the single-diode model. References [7], [14] and [33]-[38] presented methods for estimation of these 7 parameters using numerical analysis, i.e. iteration techniques and optimization methods. Due to the complexity of the equations some of the authors preferred to assume some of the parameters in order to simplify the equations. [14], [35], [38] and [39] presented a method where they assumed the ideality factor of one diode to be 1 and the other one to be 2 while [40] and [41] assumed that they are both equal to 1. This presents a reduction in accuracy of the solutions found since the assumptions made are not always applicable for all PV modules.

Other authors assumed a relationship between the reverse saturation currents of the two diodes, i.e. [38] and [42] assumed that the reverse saturation currents of the two diodes in the double-diode model are equal in magnitude to simplify the equations. Authors in [8] and [40] assumed that the second saturation current is higher than the first saturation current by five orders of magnitude and uses a relationship between the two currents derived based on that. This also simplifies the equations but at the same time compromises the accuracy of the extracted parameters since that assumption does not always apply.

All of the above described work uses the double-diode representation, with series and

shunt resistances and having 7 unknown parameters. As indicated, the approximations they make reduced the accuracy of the results.

Authors in [8] further simplified the double-diode model by neglecting the effects of the series and shunt resistances, thus reducing the number of unknown parameters to five in the double exponential equation. This reduced the computational time as well as the complexity of the modelling without really compromising on the model output. However, [8] made assumptions on the relationship of the two reverse saturation currents, hence further reducing it to 4 unknown parameters and [8] also used maximum power point matching to find the values of the two ideality factors. This reduced the accuracy of the results especially when non-STC conditions are considered.

In this study, a new improved method of extracting parameters for the simplified double-diode representation of a PV module proposed in [8] is presented. In this improved method, five unknown parameters are extracted without any assumptions, nor is any attempt to reduce the number of equations made.

3 Single-Diode model – comparative analysis

In the previous chapter, the literature relating to the different methods used in modelling of PV modules was discussed. The single-diode representation of a PV module was stated as one of the most commonly used model.

In this chapter, a comparative analysis of the different variants of the single-diode models is done based on the parameter estimation method as well as the modelling equations used for the particular model. Two parameter estimation methods are evaluated as well as five different modelling equations. The main objective of this chapter is to identify a combination of parameter estimation method as well as modelling equations which will produce the most accurate model. Accuracy of the model is evaluated by comparing the results or graphs obtained from simulations with graphs extracted from manufacturer's datasheets for KC200GT PV module as well as comparison with experimentally measured values for the SQ80 PV module. All computations are done using Matlab/Simulink software.

The single-diode representation of the PV module is described in detail in section 3.1. The two parameter estimation methods are described in detail in this section as well as the different modelling equations used. Section 3.2 outlines how simulations were done and section 3.3 describes how the experiment to take measurements was set up. Results are discussed in section 3.4 and conclusions are outlined in section 3.5.

3.1 Single-diode model

Figure 3.1 [7] shows the single-diode equivalent circuit of a PV cell. A PV module consists of a number of cells connected in series or in parallel and the relationship between the current and voltage at the terminals of the PV module is represented by (3.1) [7]:

$$I = I_{ph} - I_0 \left[\exp\left(\frac{V+IR_s}{N_s V_t}\right) - 1\right] - \frac{V+IR_s}{R_{sh}} \tag{3.1}$$

where I is the module current, V is the module voltage , I_{ph} is the photo-generated current, I_0 is the diode reverse saturation current, R_s is the series resistance, R_{sh} is the shunt resistance, N_s is the number of series connected cells in the module, V_t is the junction thermal voltage and can be expressed as $V_t = \frac{kAT}{q}$, where k is the Boltzmann's

constant equal to 1.38×10^{-23} J/K, q is the electron charge equal to 1.602×10^{-19} C and A is the diode ideality constant.

Five unknown parameters exist in (3.1), which are not available in PV module manufacturer's datasheets, i.e. I_{ph}, I_0, R_s, R_{sh} and A. The number of series connected cells, N_s is always readily available in PV module datasheets. It is therefore essential that the values of these unknown are found to complete the relationship and hence the model.

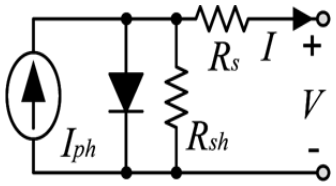

Figure 3.1 Equivalent circuit for single-diode model

3.1.1 Parameter Estimation

Two parameter estimation methods classified as method A and method B, are considered in this study. Method A uses iterative solution of equations as recommended by [20] and method B uses maximum power point matching [29]. The values obtained using these methods are valid under STC. Both parameter estimation methods consider three conditions of operation of a PV module, i.e. open circuit, short circuit and maximum power point operation. From these three conditions, five equations have to be obtained and solved in order to estimate the five unknown parameters of the single-diode model.

1. Open circuit condition

This is the condition where the output terminals of the PV module are not connected and the voltage across the PV module terminals is at its highest and equal to open circuit voltage V_{oc}. There is no current flowing at the output and thus $I = 0$.

2. Short circuit condition

This is the condition where the output terminals of the PV module are connected together (shorted) such that the voltage across the PV panel, $V = 0$. The highest value of current will flow across the PV module at this point and is equal to the short circuit current, I_{sc}.

Also under the same condition the derivative of the current with respect to voltage $\frac{dI}{dV} = \frac{-1}{R_{sho}}$ obtained from the slope of the I–V characteristic in the region closer to the

short-circuit condition, where R_{sho} is the effective resistance under short-circuit conditions. It can be shown that the assumption that $R_{sho} = R_{sh}$ is valid [7].

3. Maximum power point

At maximum power point operation, the current flowing at the output of the PV module is equal to I_{mp} and the voltage across the PV module is equal to V_{mp}.

Also, the derivative of power with respect to voltage $\frac{dP_{mp}}{dV_{mp}} = 0$ at the maximum power point.

3.1.1.1 Estimation Method A

Method A considers the three conditions of operation of a PV module as described above to come up with 5 conditions resulting in 5 equations with the 5 unknown parameters which are then solved by using an iteration method, Gaussian Iteration [20], to extract the unknown parameters.

Open circuit condition

Considering open circuit condition of operation of the PV module, that is $I = 0$ and $V = V_{oc}$ in (3.1), leads to (3.2):

$$0 = I_{ph} - I_o\left[\exp\left(\frac{V_{oc}}{N_s V_t}\right) - 1\right] - \frac{V_{oc}}{R_{sh}} \tag{3.2}$$

from which the photo-generated current can be written as (3.3):

$$I_{ph} = I_o\left[\exp\left(\frac{V_{oc}}{N_s V_t}\right) - 1\right] + \frac{V_{oc}}{R_{sh}} \tag{3.3}$$

Short-circuit condition

In considering short-circuit condition of operation of a PV module, that is $I = I_{sc}$ and $V = 0$ in (3.1), leads to (3.4):

$$I_{sc} = I_{ph} - I_o\left[\exp\left(\frac{I_{sc}R_s}{N_s V_t}\right) - 1\right] - \frac{I_{sc}R_s}{R_{sh}} \tag{3.4}$$

Also considering that the derivative of the current with respect to voltage $\frac{dI}{dV} = \frac{-1}{R_{sh}}$ under short circuit conditions [7] leads to (3.5) found by differentiating (3.1) with respect to the voltage:

$$\frac{dI}{dV} = \frac{-I_o}{N_s V_t}\left[R_s\frac{dI}{dV} + 1\right]\exp\left(\frac{V+IR_s}{N_s V_t}\right) - \frac{1}{R_{sh}} - \frac{R_s}{R_{sh}}\frac{dI}{dV} \tag{3.5}$$

Factoring like terms in (3.5) results in (3.6):

$$\frac{dI}{dV}\left[1+\frac{R_s I_o}{N_s V_t}\exp\left(\frac{V+IR_s}{N_s V_t}\right)+\frac{R_s}{R_{sh}}\right]=\frac{-I_o}{N_s V_t}\exp\left(\frac{V+IR_s}{N_s V_t}\right)-\frac{1}{R_{sh}} \tag{3.6}$$

After solving for $\frac{dI}{dV}$ in (3.6) results in (3.7):

$$\frac{dI}{dV}=\frac{\frac{-I_o}{N_s V_t}\exp\left(\frac{V+IR_s}{N_s V_t}\right)-\frac{1}{R_{sh}}}{1+\frac{R_s I_o}{N_s V_t}\exp\left(\frac{V+IR_s}{N_s V_t}\right)+\frac{R_s}{R_{sh}}} \tag{3.7}$$

Applying the relationship $\frac{dI}{dV}=\frac{-1}{R_{sh}}$ in (3.7) results in (3.8):

$$\frac{\frac{I_o}{N_s V_t}\exp\left(\frac{I_{sc}R_s}{N_s V_t}\right)+\frac{1}{R_{sh}}}{1+\frac{R_s I_o}{N_s V_t}\exp\left(\frac{I_{sc}R_s}{N_s V_t}\right)+\frac{R_s}{R_{sh}}}=\frac{1}{R_{sh}} \tag{3.8}$$

Maximum power point

At maximum power point operation, $I = I_{mp}$ and $V = V_{mp}$, and substituting these values in (3.1) results in (3.9):

$$I_{mp}=I_{ph}-I_o\left[\exp\left(\frac{V_{mp}+I_{mp}R_s}{N_s V_t}\right)-1\right]-\frac{V_{mp}+I_{mp}R_s}{R_{sh}} \tag{3.9}$$

It is also known that the derivative of power with respect to voltage, $\frac{dP_{mp}}{dV_{mp}}=0$ at the maximum power point. The derivative of power can be simplified as shown in (3.10)

$$\frac{dP_{mp}}{dV_{mp}}=\frac{d(I_{mp}V_{mp})}{dV_{mp}}=I_{mp}\frac{dV_{mp}}{dV_{mp}}+V_{mp}\frac{dI_{mp}}{dV_{mp}}=I_{mp}+V_{mp}\frac{dI_{mp}}{dV_{mp}} \tag{3.10}$$

where P_{mp} is the maximum power from the PV module under STC.

From (3.10), the derivative of power can be expressed in terms of the maximum power point current and voltage as shown in (3.11)

$$\frac{dI_{mp}}{dV_{mp}} = -\frac{I_{mp}}{V_{mp}} \tag{3.11}$$

Considering (3.7) where an expression for the derivative of current was found, substituting $I = I_{mp}$ and $V = V_{mp}$ in (3.7) and also rewriting the resulting equation in terms of I_{mp} results in (3.12):

$$I_{mp} = \frac{V_{mp}\left(\frac{I_o}{N_s V_t}\exp\left(\frac{V_{mp}+I_{mp}R_s}{N_s V_t}\right)+\frac{1}{R_{sh}}\right)}{1+\frac{R_s I_o}{N_s V_t}\exp\left(\frac{V_{mp}+I_{mp}R_s}{N_s V_t}\right)+\frac{R_s}{R_{sh}}} \tag{3.12}$$

There are now five equations, (3.3), (3.4), (3.8), (3.9) and (3.12) extracted from the three conditions of operation of a PV module which can be used to extract the five unknown parameters. Some manipulation on the equations is required to rearrange them in order to solve for the unknown parameters.

Substituting I_{ph} from (3.3) into (3.4) results in (3.13):

$$I_{sc} = I_o\left[\exp\left(\frac{V_{oc}}{N_s V_t}\right) - 1\right] + \frac{V_{oc}}{R_{sh}} - I_o\left[\exp\left(\frac{I_{sc}R_s}{N_s V_t}\right) - 1\right] - \frac{I_{sc}R_s}{R_{sh}} \tag{3.13}$$

Solving for I_o in (3.13) and also assuming that $\exp\left(\frac{V_{oc}}{N_s V_t}\right) \gg \exp\left(\frac{I_{sc}R_s}{N_s V_t}\right)$ as per [20], results in (3.14):

$$I_o = \frac{I_{sc}+\frac{I_{sc}R_s}{R_{sh}}-\frac{V_{oc}}{R_{sh}}}{\exp\left(\frac{V_{oc}}{N_s V_t}\right)-\exp\left(\frac{I_{sc}R_s}{N_s V_t}\right)} \approx \frac{I_{sc}+\frac{I_{sc}R_s}{R_{sh}}-\frac{V_{oc}}{R_{sh}}}{\exp\left(\frac{V_{oc}}{N_s V_t}\right)}$$

$$I_o = \frac{I_{sc}R_{sh}+I_{sc}R_s-V_{oc}}{R_{sh}\exp\left(\frac{V_{oc}}{N_s V_t}\right)} \tag{3.14}$$

Substituting (3.3) and (3.14) into (3.9) results in (3.15):

$$I_{mp} = \frac{I_{sc}R_{sh}+I_{sc}R_s-V_{oc}}{R_{sh}\exp\left(\frac{V_{oc}}{N_sV_t}\right)}\left[\exp\left(\frac{V_{oc}}{N_sV_t}\right) - \exp\left(\frac{V_{mp}+I_{mp}R_s}{N_sV_t}\right) + \frac{V_{oc}}{R_{sh}}\right] - \frac{V_{mp}+I_{mp}R_s}{R_{sh}} \quad (3.15)$$

Substituting (3.14) into (3.8) results in (3.16):

$$\frac{\frac{I_{sc}R_{sh}+I_{sc}R_s-V_{oc}}{N_sV_tR_{sh}\exp\left(\frac{V_{oc}}{N_sV_t}\right)}+\frac{1}{R_{sh}}}{1+\frac{R_sI_{sc}R_{sh}+R_sI_{sc}R_s-R_sV_{oc}}{N_sV_tR_{sh}}\exp\left(\frac{I_{sc}R_s-V_{oc}}{N_sV_t}\right)+\frac{R_s}{R_{sh}}} = \frac{1}{R_{sh}} \quad (3.16)$$

Substituting (3.14) into (3.12) results in (3.17):

$$I_{mp} = \frac{V_{mp}\left(\frac{I_{sc}R_{sh}+I_{sc}R_s-V_{oc}}{N_sV_tR_{sh}\exp\left(\frac{V_{oc}}{N_sV_t}\right)}\exp\left(\frac{V_{mp}+I_{mp}R_s}{N_sV_t}\right)+\frac{1}{R_{sh}}\right)}{1+\frac{R_sI_{sc}R_{sh}+R_sI_{sc}R_s-R_sV_{oc}}{N_sV_tR_{sh}\exp\left(\frac{V_{oc}}{N_sV_t}\right)}\exp\left(\frac{V_{mp}+I_{mp}R_s}{N_sV_t}\right)+\frac{R_s}{R_{sh}}} \quad (3.17)$$

There are finally five equations which can be used to solve for the five unknown parameters, and these are (3.3), (3.14), (3.15), (3.16) and (3.17).

It is also worth noting that (3.15), (3.16) and (3.17) are independent of I_{ph} and I_o and thus can be used to solve for V_t , R_{sh} and R_s using numerical methods. These values can then be used to compute the values of $I_{ph}$and $I_o$using (3.3) and (3.14) respectively.

Equation (3.15), (3.16) and (3.17) are transcendental in nature and as such they require numerical methods to find solutions to them. The Gauss-Seidel Iteration method is recommended by [20] as one which can be used to solve the three equations.

This method requires that an initial value of x^0 is selected based on known information about the solution. The next value on the iteration is calculated by using (3.18).

$$X^{k+1} = f\left(x^k\right) \quad (3.18)$$

Convergence is acquired when $x^{k+1} \approx x^{k}$, to an acceptable measure of error.
Using this iteration method requires that the equations are rearranged so that they are in the form (3.18) for the proposed method to be used.
Rearranging the terms in (3.15) results in (3.19):

$$\frac{I_{sc}R_{sh}+I_{sc}R_s-V_{oc}}{R_{sh}}\left[\exp\left(\frac{V_{mp}+I_{mp}R_s-V_{oc}}{N_sV_t}\right)-\frac{V_{oc}}{R_{sh}}\exp\left(\frac{-V_{oc}}{N_sV_t}\right)\right]=\frac{I_{sc}R_{sh}+I_{sc}R_s-V_{oc}-V_{mp}-I_{mp}R_s-I_{mp}R_s}{R_{sh}} \tag{3.19}$$

Again assuming that the term $\exp\left(\frac{V_{mp}+I_{mp}R_s-V_{oc}}{N_sV_t}\right) \gg \frac{V_{oc}}{R_{sh}}\exp\left(\frac{-V_{oc}}{N_sV_t}\right)$ as per [20] in (3.19) and solving for V_t , results in (3.20):

$$V_t=\frac{V_{mp}+I_{mp}R_s-V_{oc}}{N_s\ln\left(\frac{I_{sc}R_{sh}+I_{sc}R_s-V_{oc}-V_{mp}-I_{mp}R_s-I_{mp}R_s}{I_{sc}R_{sh}+I_{sc}R_s-V_{oc}}\right)} \tag{3.20}$$

Again, rearranging and writing (3.17) in terms of R_s, results in (3.23):

$$I_{mp}=\frac{V_{mp}\left(\frac{(I_{sc}R_{sh}+I_{sc}R_s-V_{oc})\exp\left(\frac{V_{mp}+I_{mp}R_s-V_{oc}}{N_sV_t}\right)+N_sV_t}{N_sV_tR_{sh}}\right)}{\frac{N_sV_tR_{sh}+(R_sI_{sc}R_{sh}+R_sI_{sc}R_s-R_sV_{oc})\exp\left(\frac{V_{mp}+I_{mp}R_s-V_{oc}}{N_sV_t}\right)+N_sV_tR_s}{N_sV_tR_{sh}}} \tag{3.21}$$

$$\exp\left(\frac{V_{mp}+I_{mp}R_s-V_{oc}}{N_sV_t}\right)=\frac{N_sV_tR_{sh}I_{mp}-N_sV_tV_{mp}+N_sV_tI_{mp}R_s}{(V_{mp}I_{sc}R_{sh}+V_{mp}I_{sc}R_s-V_{mp}V_{oc}+I_{mp}R_sV_{oc}-I_{mp}R_sI_{sc}R_s-I_{mp}R_sR_{sh}I_{sc})} \tag{3.22}$$

$$R_s=\frac{V_{oc}-V_{mp}+N_sV_t\ln\left[\frac{N_sV_tR_{sh}I_{mp}-N_sV_tV_{mp}+N_sV_tI_{mp}R_s}{(V_{mp}I_{sc}R_{sh}+V_{mp}I_{sc}R_s-V_{mp}V_{oc}+I_{mp}R_sV_{oc}-I_{mp}R_sI_{sc}R_s-I_{mp}R_sR_{sh}I_{sc})}\right]}{I_{mp}} \tag{3.23}$$

Rearranging and writing (3.16) in terms of R_{sh} results in (3.26):

$$\frac{\frac{(I_{sc}R_{sh}+I_{sc}R_s-V_{oc})\exp\left(\frac{I_{sc}R_s-V_{oc}}{N_sV_t}\right)}{N_sV_tR_{sh}}+\frac{1}{R_{sh}}}{1+\frac{R_sI_{sc}R_{sh}+R_sI_{sc}R_s-R_sV_{oc}}{N_sV_tR_{sh}}\exp\left(\frac{I_{sc}R_s-V_{oc}}{N_sV_t}\right)+\frac{R_s}{R_{sh}}}=\frac{1}{R_{sh}} \tag{3.24}$$

$$\frac{\frac{(I_{sc}R_{sh}+I_{sc}R_s-V_{oc})\exp\left(\frac{I_{sc}R_s-V_{oc}}{N_sV_t}\right)+N_sV_t}{N_sV_tR_{sh}}}{\frac{N_sV_tR_{sh}+(R_sI_{sc}R_{sh}+R_sI_{sc}R_s-R_sV_{oc})\exp\left(\frac{I_{sc}R_s-V_{oc}}{N_sV_t}\right)+N_sV_tR_s}{N_sV_tR_{sh}}} = \frac{1}{R_{sh}} \tag{3.25}$$

$$R_{sh} = \frac{N_sV_tR_{sh}+(R_sI_{sc}R_{sh}+R_sI_{sc}R_s-R_sV_{oc})\exp\left(\frac{I_{sc}R_s-V_{oc}}{N_sV_t}\right)+N_sV_tR_s}{(I_{sc}R_{sh}+I_{sc}R_s-V_{oc})\exp\left(\frac{I_{sc}R_s-V_{oc}}{N_sV_t}\right)+N_sV_t} \tag{3.26}$$

In summary, initial values are assigned based on the best estimation possible for that particular parameter and in this case initial value for $R_s = 0$ based on the ideal case and for $R_{sh} = 1000$ based on the fact that in the ideal case the shunt resistance is assumed to be equal to infinity and using these initial values, the initial value for V_t is calculated from (3.20).

Using these initial values, the next set of values are calculated for all parameters. If the calculated error based on the difference between the current and previous values is within the chosen tolerance (0.1%), then the current value is taken as the solution and the iteration stops. It is expected that after a few iterations, the equations will converge to a solution. A matlab code is written to implement these steps, as shown in Appendix B. The matlab function takes parameters from the datasheet of a PV module and returns the five parameters, I_{ph}, I_o, V_t, R_s and R_{sh}.

3.1.1.2 Estimation Method B

Parameter estimation method B involves reducing the number of equations to 4 by estimating one of the parameters while comparing the maximum power point as recommended by [29] and [31]. The same idea was used by [24] where the ideality factor is perturbed instead of the series resistance. The equations in this method are also derived from the three operating conditions of the PV module mentioned at the beginning of section 3.1.1.

Considering short circuit conditions, in this method it is assumed that the second term on the right hand side of (3.4) is small compared to the first and second term, that is $I_{ph} - \frac{I_{sc}R_s}{R_{sh}} \gg I_o\left[\exp\left(\frac{I_{sc}R_s}{N_sV_t}\right) - 1\right]$ [29], such that it can be neglected resulting in (3.27).

$$I_{ph,STC} = \frac{R_s+R_{sh}}{R_{sh}} I_{sc} \tag{3.27}$$

The next step is to derive an expression for the ideality factor. Considering open circuit conditions and the assumption that the shunt resistances is very high in (3.2) results in (3.28):

$$0 = I_{ph} - I_o \left[\exp\left(\frac{V_{oc}}{AN_sV_t}\right) - 1\right] \approx I_{ph} - I_o \exp\left(\frac{V_{oc}}{AN_sV_t}\right) \tag{3.28}$$

Solving for V_{oc} in (3.28) results in (3.29):

$$V_{oc} = -AN_sV_t \ln\left(\frac{I_o}{I_{ph}}\right) \tag{3.29}$$

The open circuit voltage temperature coefficient can be calculated as follows:

$$K_v = \frac{dV_{oc}}{dT} = \frac{d}{dT}\left[AN_sV_t \ln I_{ph} - AN_sV_t \ln I_o\right] \tag{3.30}$$

Considering that the thermal voltage $V_t = \frac{kT}{q}$ and also that the reverse saturation current $I_o = DT^3 \exp\left(-\frac{qE_g}{kT}\right)$, where D is an arbitrary constant dependent on the diffusion properties of the junction [43], depend on temperature we have (3.31)

$$K_v = \frac{AN_sV_t}{T} \ln\left(\frac{I_{ph}}{I_o}\right) + AN_sV_t \left[\frac{1}{I_{ph}} \frac{dI_{ph}}{dT} - \frac{1}{I_o} \frac{dI_o}{dT}\right] \tag{3.31}$$

The second term in the brackets in (3.31) can be calculated as

$$\frac{1}{I_o} \frac{dI_o}{dT_{STC}} = \frac{3}{T_{STC}} + \frac{qE_g}{kT_{STC}^2} \tag{3.32}$$

The first term is related to the current, thus

$$K_v = \frac{AN_sV_t}{T} \ln\left(\frac{I_{ph}}{I_o}\right) + AN_sV_t \left[\frac{K_i}{I_{ph}} - \frac{3}{T_{STC}} + \frac{qE_g}{kT_{STC}^2}\right] \tag{3.33}$$

This can also be written as

$$K_v = \frac{V_{oc}}{T_{STC}} + AN_sV_t \left[\frac{K_i}{I_{ph}} - \frac{3}{T_{STC}} + \frac{qE_g}{kT_{STC}^2}\right] \tag{3.34}$$

Making A the subject in (3.34) results in (3.35)

$$A = \frac{K_v - \frac{V_{oc}}{T_{STC}}}{N_s V_T \left(\frac{K_I}{I_{ph,STC}} - \frac{3}{T_{STC}} - \frac{qE_g}{kT_{STC}^2} \right)} \tag{3.35}$$

In the above equation (3.35), $V_t = \frac{kT_{STC}}{q}$ and the value of E_g can be calculated using (3.36) [7]:

$$E_g = E_{go} - \frac{\gamma T^2}{\beta + T} \tag{3.36}$$

where E_{go}, γ and β are fitting parameters as listed in table 3.1, K_v and K_I are the temperature coefficients for voltage and current respectively.

Table 3.1: Fitting parameters for crystalline cells

	Germanium	**Silicon**	**GaAs**
E_{go}(eV)	0.7437	1.166	1.519
γ (eV/K)	4.77 x 10^{-4}	4.73 x 10^{-4}	5.41 x 10^{-4}
β (eV/K)	235	636	204

The reverse saturation current I_o in this method is calculated by using (3.14) as will be shown during the iteration procedure.

According to [29], the value of shunt resistance can be approximated as the slope of the line segment between the short circuit point and the maximum power point of the I-V characteristic. This is the value of shunt resistance R_{sh} which will be taken as the initial value and can be calculated using (3.37):

$$R_{sh(in)} = \frac{V_{mp}}{I_{sc} - I_{mp}} - \frac{V_{oc} - V_{mp}}{I_{mp}} \tag{3.37}$$

For calculating subsequent values for R_{sh} during the iteration, maximum power operation is considered. The maximum power from the PV module is the product of the voltage and the current at the maximum power point and an expression for the maximum power is as shown in (3.39) obtained by multiplying the maximum power point current equation (3.9) by V_{mp} resulting in (3.38).

$$P_{max} = V_{mp} I_{mp} = V_{mp} \left\{ I_{ph} - I_o \left[\exp\left(\frac{V_{mp} + I_{mp} R_s}{N_s V_t} \right) - 1 \right] - \frac{V_{mp} + I_{mp} R_s}{R_{sh}} \right\} \tag{3.38}$$

or

$$P_{max} = V_{mp}\left\{I_{ph} - I_o\left[\exp\left(\frac{V_{mp}+I_{mp}R_s}{N_s V_t}\right) - 1\right] - \frac{V_{mp}+I_{mp}R_s}{R_{sh}}\right\} \quad (3.39)$$

Solving for R_{sh} in (3.39) results in (3.40):

$$R_{sh} = \frac{V_{mp}(V_{mp}+I_{mp}R_s)}{V_{mp}I_{ph}+V_{mp}I_o-P_{max}-V_{mp}I_o\exp\left(\frac{q(V_{mp}+I_{mp}R_s)}{N_s kAT}\right)} \quad (3.40)$$

This method involves perturbation of the value of R_s in small incrementing steps. At each step, all the parameters are calculated as well as the value of the maximum power which is compared with the value given in the PV model's datasheet. This is done until the calculated value of maximum power is within an acceptable error (0.1%) when compared with the value given in the datasheet. A flow chart showing the steps followed in implementing this method is illustrated in Figure 3.2 [29]. The computation of this algorithm was also done in a matlab code as shown in appendix C. The matlab function takes parameters from the datasheet of a PV module and returns the five parameters, I_{ph}, I_o, V_t, R_s and R_{sh}.

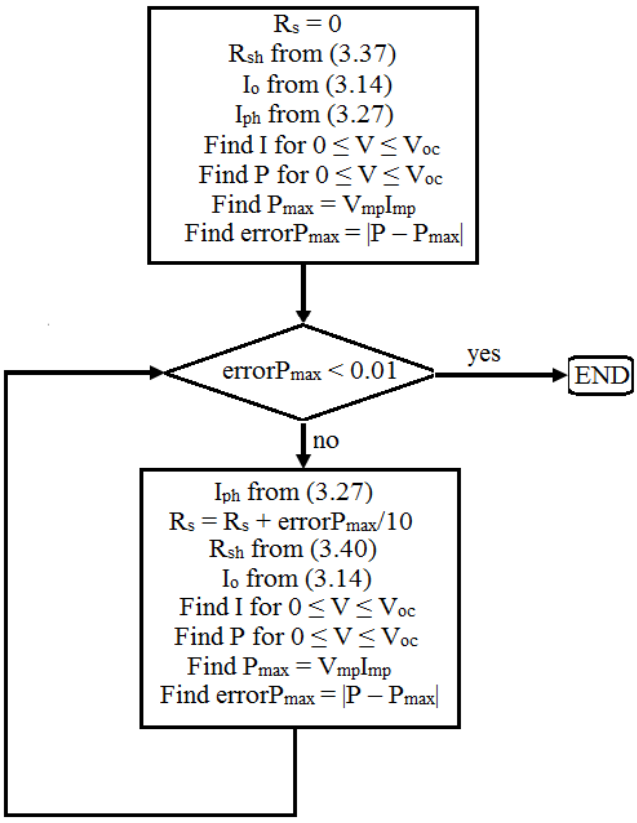

Figure 3.2. Algorithm for parameter estimation in method B

3.1.2 Different Modelling Equations

The operation of PV arrays is normally under changing atmospheric conditions which will be affected by the overall irradiance and temperature under which the PV array is operated. These conditions have an effect on the overall output of the PV array. It is therefore essential that they are considered during the modelling of the PV module. Most of the modelling work considers that the ideality factor, the series resistance and the shunt resistance are constant with varying temperature thus they are assumed not to change with temperature [28].

The only parameters which are considered to change with both temperature and irradiance are I_o and I_{ph}. A modelling technique is made up by a combination of equations to evaluate these two parameters as functions of temperature and irradiance. Five combinations of equations are identified in literature for all single-diode mathematical models that are classified as model 1, model 2, model 3, model 4 and model 5 in this study.

3.1.2.1 Model 1 [20], [27]

Model 1 considers the temperature dependence of I_{sc} and V_{oc} as shown in (3.41) and (3.42).

$$V_{oc}(T) = V_{oc} + K_v \Delta T \tag{3.41}$$

$$I_{sc}(T) = I_{sc} + K_I \Delta T \tag{3.42}$$

The equations (3.14) and (3.3) can be rewritten as (3.43) and (3.44) respectively:

$$I_o = \frac{\left(I_{sc,STC} + K_I(T-298)\right)R_s + \left(I_{sc,STC} + K_I(T-298)\right)R_{sh} - \left(V_{oc,STC} + K_V(T-298)\right)}{R_{sh}\exp\left(\frac{\left(V_{oc,STC} + K_V(T-298)\right)}{N_s V_t}\right)} \tag{3.43}$$

$$I_{ph} = G\left[I_o\left\{\exp\left(\frac{(V_{oc} + K_v \Delta T)}{N_s V_t}\right) - 1\right\} + \frac{V_{oc} + K_v \Delta T}{R_{sh}}\right] \tag{3.44}$$

where T is the temperature of the module, ΔT is the temperature difference $T - T_{STC}$, T_{STC} is the temperature at STC which is equal to 298K and G is the ratio of the irradiance

with respect to STC value (i.e. 1kW/m^2).

3.1.2.2 Model 2 [11], [29], [31]

If we consider $I_{ph,STC} = I_{sc}$ and also that the resistance R_{sh} is very high so that the second term on the right of (3.3) becomes zero and rearranging we get (3.45):

$$I_o = \frac{I_{sc}}{\exp\left(\frac{(V_{oc})}{N_s V_t}\right)-1} \tag{3.45}$$

Also Considering the temperature dependence of I_{sc} and V_{oc} given in (3.41) and (3.42), (3.45) can be rewritten as (3.46):

$$I_o = \frac{I_{sc}+K_I\Delta T}{\exp\left(\frac{(V_{oc}+K_V\Delta T)}{N_s V_t}\right)-1} \tag{3.46}$$

The photo generated current of every PV module is said to vary with respect to the irradiance as well as the temperature by the relation shown in (3.47) [34].

$$I_{ph} = (I_{ph,STC} + K_I\Delta T)G \tag{3.47}$$

3.1.2.3 Model 3 [21], [25]

In this model, it is assumed that $I_{ph,STC} = I_{sc}$, making I_o the subject in (3.3) results in (3.48):

$$I_{o,STC} = \frac{I_{ph,STC}-\frac{V_{oc}}{R_{sh}}}{\exp\left(\frac{V_{oc}}{N_s V_t}\right)-1} \tag{3.48}$$

Considering that the resistance R_{sh} is very high such that (3.48) becomes (3.49):

$$I_{o,STC} = \frac{I_{ph,STC}}{\exp\left(\frac{V_{oc}}{N_s V_t}\right)-1} \tag{3.49}$$

Making V_{oc} the subject of the formula in (3.49) and considering that $V_t = \frac{kAT}{q}$ we get (3.50):

$$V_{oc} = \frac{N_s kTA}{q}\ln\left(\frac{I_{ph,STC}}{I_{o,STC}} + 1\right) \tag{3.50}$$

Using the fact that $V_{oc}(G,T) - V_{oc}(G,T_{STC}) = -|K_V|\Delta T$ and that $I_{ph} = (I_{sc} + K_i\Delta T)G$:

$$\frac{N_s kTA}{q}\left[T\ln\left(\frac{G(I_{sc}+K_I\Delta T)}{I_o} + 1\right) - T_{STC}\ln\left(\frac{GI_{sc}}{I_{o,STC}} + 1\right)\right] = -|K_V|\Delta T \tag{3.51}$$

(3.51) can be written in terms of the reverse saturation current resulting in (3.52)

$$I_o = \frac{G(I_{sc}+K_I\Delta T)\exp\left(\frac{q|K_V|\Delta T}{N_S kTA}\right)}{\left(\frac{GI_{sc}}{I_{o,STC}}+1\right)^{\frac{T_{STC}}{T}} - \exp\left(\frac{q|K_V|\Delta T}{N_S kTA}\right)} \quad (3.52)$$

To calculate the photo generated current in this model, (3.47) is used. Considering the assumption that $I_{ph,STC} = I_{sc}$ leads to (3.53).

$$I_{ph} = (I_{sc} + K_I\Delta T)G \quad (3.53)$$

3.1.2.4 Model 4 [7], [40]

In this model it is considered that the saturation current is related to the band gap and temperature by (3.54) below

$$I_o = DT^3\exp\left(\frac{-qE_g}{AkT}\right) \quad (3.54)$$

where D is a constant dependent on the diffusion properties of the junction and E_g is the band gap energy [43]. Evaluating (3.54) at temperature T_{STC} and T results in (3.55) and (3.56) respectively.

$$I_{o,STC} = DT_{STC}^3\exp\left(\frac{-qE_g}{AkT_{STC}}\right) \quad (3.55)$$

$$I_o = DT^3\exp\left(\frac{-qE_g}{AkT}\right) \quad (3.56)$$

Taking the ratio of (3.55) and (3.56) and rearranging results in (3.57).

$$I_o = I_{o,STC}\left[\frac{T}{T_{STC}}\right]^3\exp\left(\frac{qE_g}{Ak}\left(\frac{1}{T_{STC}} - \frac{1}{T}\right)\right) \quad (3.57)$$

To calculate the photo generated current in this model, (3.47) is used.

3.1.2.5 Model 5 [24]

Model 5 uses (3.1) under open circuit conditions, $I = 0$ and $V = V_{oc}$, and rearranging leading to (3.58).

$$I_{ph,STC} = I_{o,STC}\left[\exp\left(\frac{V_{oc}}{N_S V_t}\right) - 1\right] + \frac{V_{oc}}{R_{sh}} \quad (3.58)$$

Also using (3.1) under short circuit conditions, $I = I_{sc}$ and $V = 0$, leads to (3.59)

$$I_{sc} = I_{ph,STC} - I_{o,STC}\left[\exp\left(\frac{I_{sc}R_s}{N_sV_t}\right) - 1\right] - \frac{I_{sc}R_s}{R_{sh}} \tag{3.59}$$

Substituting for $I_{ph,STC}$ in (3.58) into (3.59) and rearranging leads to (3.60)

$$I_{o,STC} = \frac{\left(1+\frac{R_s}{R_{sh}}\right)I_{sc} - \frac{V_{oc}}{R_{sh}}}{\exp\left(\frac{V_{oc}}{N_sV_t}\right) - \exp\left(\frac{I_{sc}R_s}{N_sV_t}\right)} \tag{3.60}$$

Considering temperature dependence of I_{sc} and V_{oc}, a new equation relating $V_{oc}(T)$ to the STC value is derived [24]. The open circuit conditions are considered and also that $\exp\left(\frac{V_{oc}}{N_sV_t}\right) \gg 1$ in (3.2), and this results in (3.61).

$$0 = I_{ph} - I_o\exp\left(\frac{V_{oc}}{N_sV_t}\right) - \frac{V_{oc}}{R_{sh}} \tag{3.61}$$

Rearranging (3.61) results in (3.62)

$$V_{oc} = N_sV_t\ln\left(\frac{I_{ph}R_{sh} - V_{oc}}{I_oR_{sh}}\right) \tag{3.62}$$

Usually the shunt resistance is high such that $I_{ph}R_{sh} \gg V_{oc}$, as a result the second term is neglected so that (3.62) becomes (3.63)

$$V_{oc} = N_sV_t\ln\left(\frac{I_{ph}}{I_o}\right) \tag{3.63}$$

Evaluating (3.63) at STC conditions assuming that (3.63) is at non STC conditions results in (3.64)

$$V_{oc,STC} = N_sV_t\ln\left(\frac{I_{ph,STC}}{I_{o,STC}}\right) \tag{3.64}$$

The difference between (3.63) and (3.64) can be expressed as (3.65)

$$V_{oc} - V_{oc,STC} = N_sV_t\ln\left(\frac{I_{ph}}{I_o}\right) - N_sV_t\ln\left(\frac{I_{ph,STC}}{I_{o,STC}}\right) \tag{3.65}$$

After some mathematical manipulations on (3.65), (3.66) is obtained

$$V_{oc} - V_{oc,STC} = N_sV_t\ln\left(\frac{I_{ph}}{I_{ph,STC}}\right) \tag{3.66}$$

Lastly considering the fact that the photo-generated current is directly proportional to the irradiance, meaning that the ratio $\frac{I_{ph}}{I_{ph,STC}}$ can be equated to the irradiance G, (3.66) can be written as (3.67)

$$V_{oc}(T) = V_{oc} + K_v\Delta T + V_t\ln(G) \tag{3.67}$$

It is considered that there is dependence of V_{oc} on the irradiance hence the inclusion of the logarithmic factor in the equation. Substituting for I_{ph} in (3.3) into (3.4) and

rearranging results in (3.68).

$$I_o = \frac{\left(1+\frac{R_s}{R_p}\right)I_{sc} - \frac{V_{oc}}{R_p}}{\exp\left(\frac{V_{oc}}{V_t}\right) - \exp\left(\frac{I_{sc}R_s}{V_t}\right)} \tag{3.68}$$

And consequently substituting (3.41) for I_{sc} and (3.42) for V_{oc} in (3.68), results in the (3.69):

$$I_o = \frac{\left(1+\frac{R_s}{R_p}\right)(I_{sc}+K_I\Delta T) - \frac{V_{oc}+K_V\Delta T+V_t\ln(G)}{R_p}}{\exp\left(\frac{V_{oc}+K_V\Delta T+\ln(G)}{V_t}\right) - \exp\left(\frac{(I_{sc}+K_I\Delta T)R_s}{V_t}\right)} \tag{3.69}$$

In this model, the photo generated current is calculated using (3.47).

3.2 Simulations

In the previous section parameter estimation method A and method B were described in detail as well as the different models: model 1, model 2, model 3, model 4 and model 5. This section describes the simulations which were done for all the models.

Matlab Simulink was used to simulate and plot the I-V characteristic graphs based on the different models. The block labelled "METHOD A" in figure A.1 (in Appendix A) is embedded with the Matlab code for estimating the five unknown parameters using method A is shown in appendix A and the Matlab code for estimating the five unknown parameters using method B is shown in appendix B.

Figure 3.3 shows the Matlab Simulink function block used to represent the equations for model 1 as well as the Matlab function code embedded in the Simulink block. The function takes the STC values for R_s, R_{sh}, I_{sc}, V_{oc}, K_I, K_V and A as inputs. It also takes N_s as well as T and G. The outputs of the function are I_o, I_{ph} and V_t, which are parameters dependent on the temperature T and irradiance G. I_o is calculated using (3.43) and I_{ph} is calculated using (3.44).

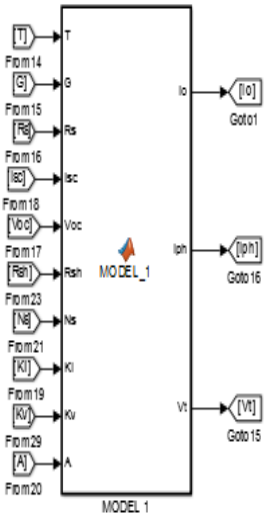


```
function [Io, Iph, Vt] = MODEL_1( T, G, Rs, Isc, Voc, Rsh, Ns, Ki, Kv, A)
%Function evaluates the output parameters Io, Iph and Vt at a specific
%temperature and irradiance by using MODEL 1 equations.


q=1.602e-19;  % declare electron charge
K=1.38e-23;   % declare Boltzman's constant


Vt=K*T*A/q;   % calculate Vt(T)

Io=((Isc+Ki*(T-298))*Rsh+(Isc+Ki*(T-298))*Rs-(Voc+Kv*(T-298)))/(Rsh*exp((Voc+Kv*(T-298))/(Ns*Vt)));
Iph=(Io*(exp((Voc+Kv*(T-298))/(Ns*Vt))-1)+((Voc+Kv*(T-298))/Rsh))*G;


end
```

Figure 3.3 Simulink function block and Matlab code for Model 1 equations

Figure 3.4 shows the Matlab Simulink function block used to represent the equations for model 2 as well as the Matlab function code embedded in the Simulink block. The function takes the STC values for R_s, R_{sh}, I_{sc}, V_{oc}, K_I, K_V and A as inputs. It also takes N_s as well as T and G. The outputs of the function are I_o, I_{ph} and V_t, which are parameters dependent on the temperature T and irradiance G. I_o is calculated using (3.46) and I_{ph} is calculated using (3.47).

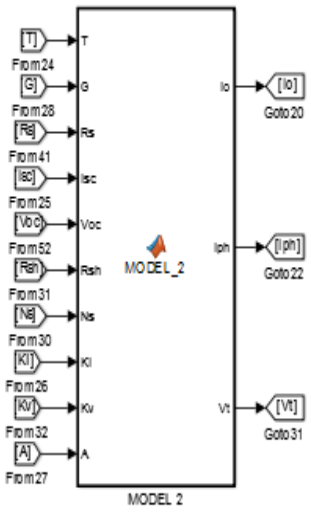


```
function [Io, Iph, Vt] = MODEL_2( T, G, Rs, Isc, Voc, Rsh, Ns, Ki, Kv, A)
%Function evaluates the output parameters Io, Iph and Vt at a specific
%temperature and irradiance by using MODEL 2 equations.


q=1.602e-19;  % declare electron charge
K=1.38e-23;   % declare Boltzman's constant


Vt=K*T*A/q;   % calculate Vt(T)

Iphn=((Rsh+Rs)/Rsh)*Isc;
Io=(Isc+Ki*(T-298))/(exp((Voc+Kv*(T-298))/(Ns*Vt))-1);
Iph=(Iphn+Ki*(T-298))*G;


end
```

Figure 3.4 Simulink function block and Matlab code for Model 2 equations

Figure 3.5 shows the Matlab Simulink function block used to represent the equations for model 3 as well as the Matlab function code embedded in the Simulink block. The function takes the STC values for R_s, R_{sh}, I_{sc}, I_{on}, K_I, K_V and A as inputs, I_{on} is the STC value for the reverse saturation current. It also takes N_s as well as T and G. The outputs of the function are I_o, I_{ph} and V_t, which are parameters dependent on the temperature T and irradiance G. I_o is calculated using (3.52) and I_{ph} is calculated using (3.53).

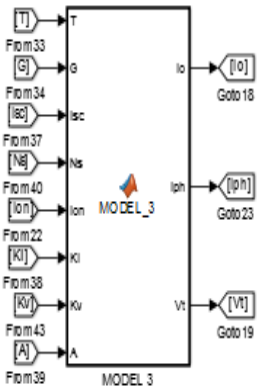


```
function [Io, Iph, Vt] = MODEL_3( T, G, Isc, Ns, Ion, Ki, Kv, A)
%Function evaluates the output parameters Io, Iph and Vt at a specific
%temperature and irradiance by using MODEL 3 equations.

q=1.602e-19;  % declare electron charge
K=1.38e-23;   % declare Boltzman's constant
Vt=K*T*A/q;   % calculate Vt(T)

Iphn=Isc;
Io = (G*(Isc+Ki*(T-298))*exp(abs(Kv)*(T-298)*q/(Ns*K*T*A)))/((((G*Isc/Ion)+1)^(298/T))-exp(abs(Kv)*(T-298)*q/(Ns*K*T*A)));
Iph=(Iphn+Ki*(T-298))*G;

end
```

Figure 3.5 Simulink function block and Matlab code for Model 3 equations

Figure 3.6 shows the Matlab Simulink function block used to represent the equations for model 4 as well as the Matlab function code embedded in the Simulink block. The function takes the STC values for R_s, R_{sh}, I_{phn}, I_{on}, K_I and A as inputs where the subscript n is used to denote STC parameters, I_{phn} is the STC value for the photo-generated current and I_{on} is the STC value for the reverse saturation current It also takes

N_s as well as T and G. The outputs of the function are I_o, I_{ph} and V_t, which are parameters dependent on the temperature T and irradiance G. I_o is calculated using (3.57) and I_{ph} is calculated using (3.47).

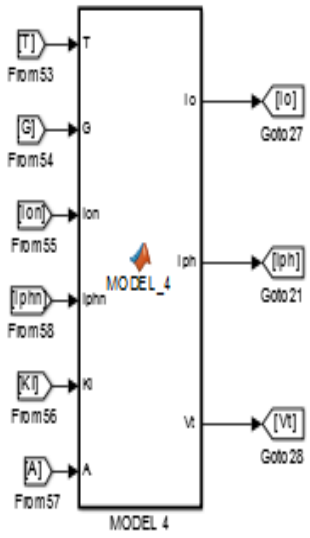


```
function [Io, Iph, Vt] = MODEL_4( T, G, Ion, Iphn, Ki, A)
%Function evaluates the output parameters Io, Iph and Vt at a specific
%temperature and irradiance by using MODEL 4 equations.
q=1.602e-19;    % declare electron charge
K=1.38e-23;     % declare Boltzman's constant
Ego=1.166;      % assign fitting parameter for silicon
B=636;          % assign fitting parameter for silicon
M=4.7e-4;       % assign fitting parameter for silicon

Vt=K*T*A/q;     % calculate Vt(T)
Eg=Ego-((M*T^2)/(T+B));  % calculate Eg(T)

Io = Ion*((T/298)^3)*exp((q*Eg/(A*K))*((1/298)-(1/T)));
Iph=(Iphn+Ki*(T-298))*G;

end
```

Figure 3.6 Simulink function block and Matlab code for model 4 equations

Figure 3.7 shows the Matlab Simulink function block used to represent the equations for model 5 as well as the Matlab function code embedded in the Simulink block. The function takes the STC values for R_s, R_{sh}, I_{phn}, I_{sc}, V_{oc} , K_I and A as inputs, I_{phn} is the STC value for the photo-generated current. It also takes N_s as well as T and G. The outputs of the function are I_o, I_{ph} and V_t, which are parameters dependent on the temperature T and irradiance G. I_o is calculated using (3.69) and I_{ph} is calculated using (3.47).

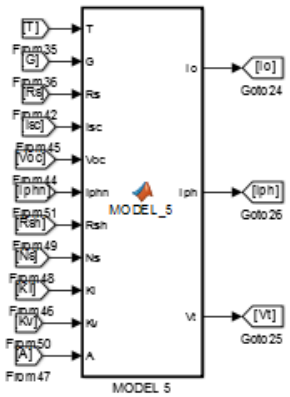


```
function [Io, Iph, Vt] = MODEL_5( T, G,Rs,Isc,Voc, Iphn, Rsh, Ns, Ki,Kv, A)
%Function evaluates the output parameters Io, Iph and Vt at a specific
%temperature and irradiance by using MODEL 1 equations.

q=1.602e-19;   % declare electron charge
K=1.38e-23;    % declare Boltzman's constant

Vt=K*T*A/q;    % calculate Vt(T)

Io=(((Rsh+Rs)/Rsh)*(Isc+Ki*(T-298))-((Voc+Kv*(T-298)+Vt*log(G))/Rsh))/(exp
((Voc+Kv*(T-298)+Vt*log(G))/(Ns*Vt))-exp((Isc+Ki*(T-298))*Rs/(Ns*Vt)));
Iph=(Iphn+Ki*(T-298))*G;


end
```

Figure 3.7 Simulink function block and Matlab code for Model 5 equations

Figure 3.8 shows the Simulink block which evaluates the PV module's current for values of V ranging from zero to V_{oc}. The input voltage is shown as a ramp input into the Simulink block. The function block labelled Fcn in figure 3.8 is embedded with a function for calculating the PV output current using equation (3.1).

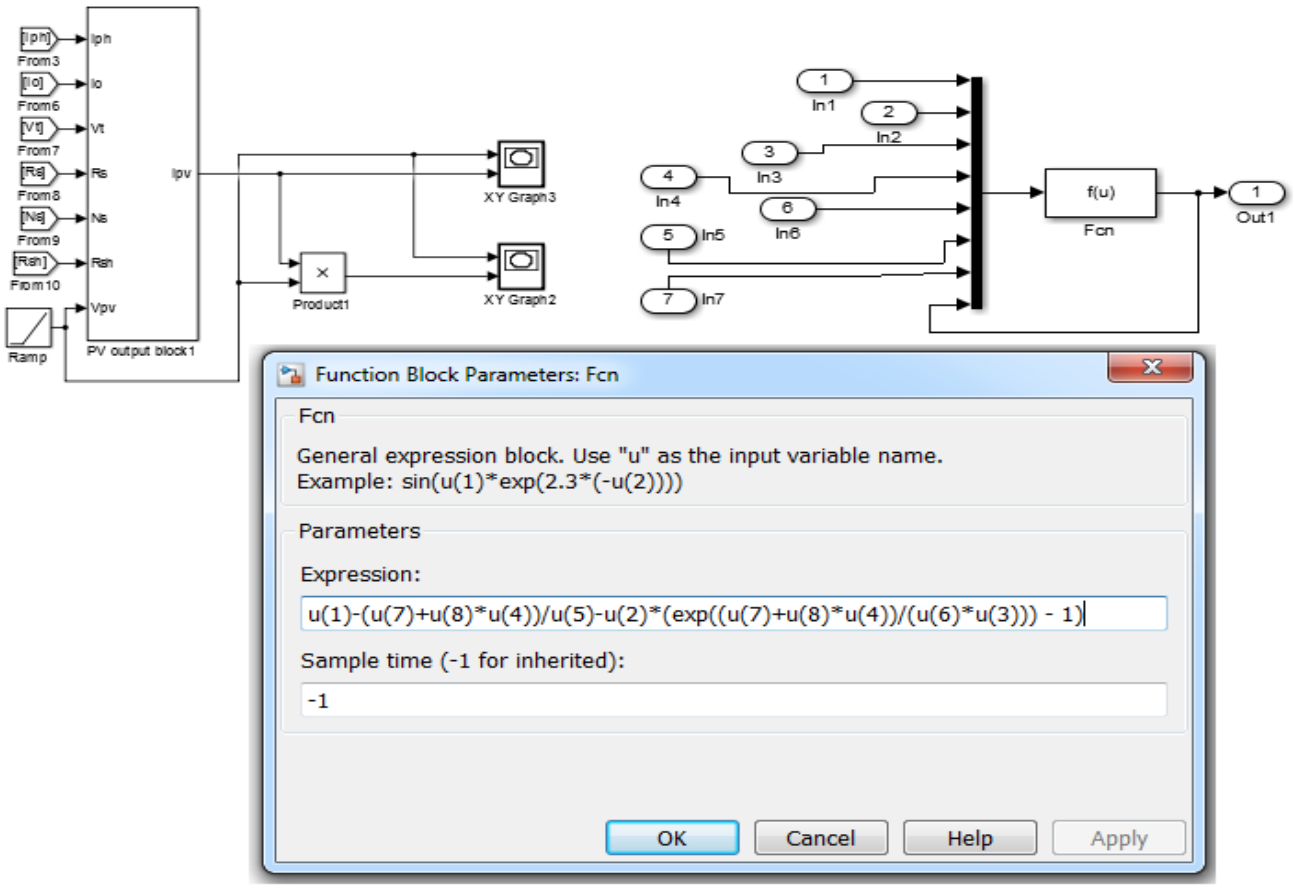

Figure 3.8 Simulink block for calculation of PV output current for single-diode model

3.3 Experimental setup

In section 3.2 the different Simulink blocks and Matlab code which were used to produce simulation results for the two PV modules were outlined. In this section, a description of how the experimental measurements from the SQ80 PV module were taken.

Experimental measurements were taken using the SQ80 module connected to the PVPM curve plotter. The setup is shown in figure 3.9.

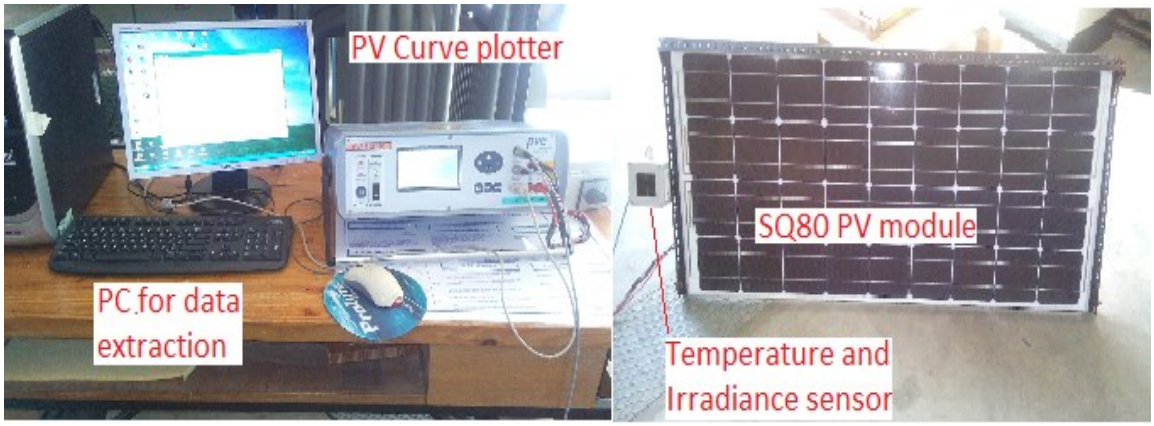

Figure 3.9 Experimental setup used to take measurements from SQ80 PV module.

It consists of the SQ80 PV module with a temperature and irradiance sensor attached to it. It is assumed that the recorded temperature and irradiance is the same as the one on the PV module. The module and sensors are connected to the PVPM2540-C curve plotter using cables. A PC is connected to the curve plotter via a serial connection and is used to extract the readings from the PVPM2540-C curve plotter. The PVPM automatically measures the I-V characteristic of the PV module at a capacitive load. From the measurement data it calculates the effective solar cell characteristic. The measured data is stored automatically in a non-volatile storage. This data can then be extracted and stored in excel format in the connected PC. This also enables the increase in number of measurements taken since the PVPM can only store a maximum of 100 readings.

In this study the PVPM curve plotter was configured to take data samples every 30 seconds for one day on the 18th November 2014. The first reading was taken at 10h48 and the last one was taken at 17h28. At each sampling instance, it measured a full set of readings for current, voltage, temperature and irradiance, then transferred the data to the connected PC via a serial interface, and as expected the values of irradiance and temperature varied over the duration of the recording interval. The recorded readings were analysed and selected such that the set of data corresponding to the relevant desired conditions, i.e. fixed temperature at different irradiance values or fixed irradiance at different temperatures were then selected and used.

There was a margin of error allowed in selecting the set of measurements corresponding to ±0.05kW/m^2 for irradiance and ±3°C for the temperature. This margin of error is acceptable considering the small temperature coefficients of the SQ80 PV module as shown in table 3.2. The experimental readings were extracted and included

in the simulation plots for comparison. Table D.1 in appendix D shows measured values of voltage and current at 1kW/m^2 under varying temperature and table D.2 in appendix D shows measured values for voltage and current under varying irradiance at a temperature of 25 °C. It should be noted that the curve plotter datasheet indicates an uncertainty of peak power measurement and A/D converter accuracy as+/−5% and+/−0.25%, respectively.

3.4 Results and Discussion

In this section the simulation results will be outlined and discussed to provide a comparison of the parameter estimation methods: method A and method B, as well as a comparison of the different modelling equations (Models 1 to 5).

The Shell SQ80 [44] and KC200GT [45] modules whose datasheet parameters specified under STC are given in table 3.2 were used to evaluate and test the different modelling methods discussed in the previous section.

Table 3.2 Datasheet Parameters for PV modules

Parameter	SQ80	KC200GT
N_s	36	54
I_{sc}	4.85A	8.21A
V_{oc}	21.8V	32.9V
V_{mp}	17.5V	26.3V
I_{mp}	4.58A	7.61A
K_I	0.0014A/°C	0.00318A/°C
K_V	-0.081V/°C	-0.123V/°C

The parameters estimated using the two parameter estimation methods for the two PV modules are shown in table 3.3 and table 3.4.

Table 3.3 SQ80 STC Parameters Estimated using Method A and Method B

Parameter	Estimated value	
	Method A	**Method B**
R_s	0.3763Ω	0.3085Ω
R_{sh}	1.005kΩ	1.676 kΩ
V_t	0.0243V	0.02739V
I_o	6.967×10^{-11}	1.207×10^{-9}
I_{ph}	4.8518A	4.85A
A	0.95	1.067

Table 3.4 KC200GT STC Parameters Estimated using Method A and Method B

Parameter	Estimated value	
	Method A	**Method B**
R_s	0.2163Ω	0.29Ω
R_{sh}	993.0Ω	160.3Ω
V_t	0.0345V	0.02739V
I_o	1.772×10^{-7}A	2.179×10^{-9}A
I_{ph}	8.212A	8.21A
A	1.343	1.067

The graphs shown in figure 3.10 and figure 3.11 depict the results under varying irradiance for all five models using method A and method B respectively, and also includes plots using experimentally measured data for the SQ80 module.

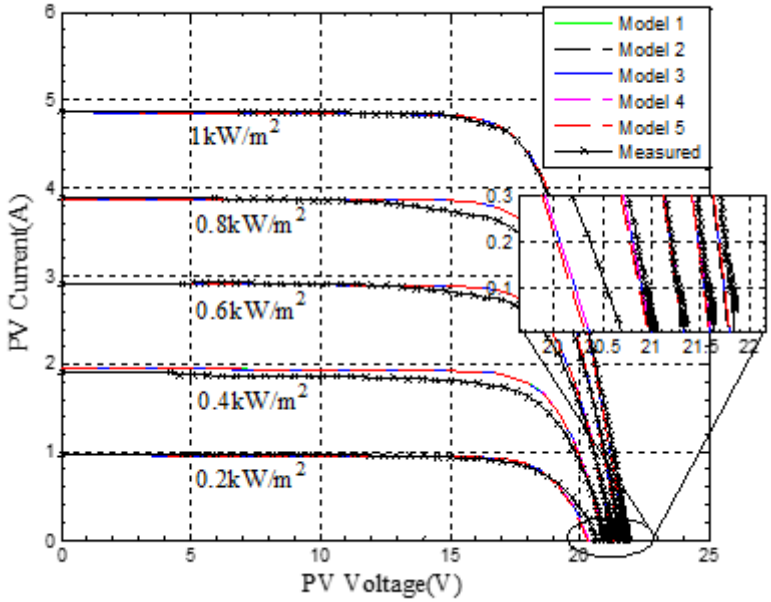

Figure 3.10 I-V Characteristic for SQ80 module under varying irradiance for models 1, 2,3,4,5 and measured values, using parameter estimation method A

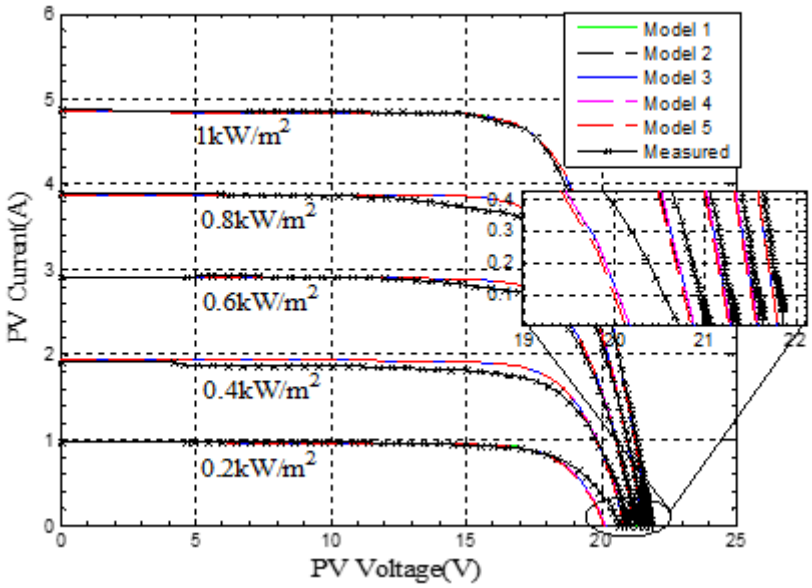

Figure 3.11 I-V Characteristic for SQ80 module under varying irradiance for model 1, 2, 3, 4, 5 and measured values, using parameter estimation method B

The graphs in figure 3.10 and figure 3.11 show that the open circuit voltage response to changes in irradiance is the same for all the modelling methods described in this study. In the equation (3.71) for saturation current in model 5, a factor was introduced which is meant to cater for dependence of open circuit voltage on the irradiance. In inclusion of this factor, [24] explained that there is a logarithmic dependence between the voltage and the irradiance, but figure 3.10 and figure 3.11 clearly show that the dependence of open circuit voltage on irradiance is minimal for the single-diode model.

The similarity of the short circuit current response from all models was expected since in all the recommended modelling methods, the equation used for calculating I_{ph} is the same except for model 1. In comparison to the plot using experimental values, it can be seen that the response in terms of the short circuit values is the same for both plots again owing to the comparable results found for I_{ph} using the two methods. However, considering the response as far as the open circuit voltage is concerned, a small difference can be seen from the two plots and the graph which shows results closer to the experimental results is the one in figure 3.10, using method A to estimate parameters. Table 3.5 gives a clear summary of the variation of the open circuit voltage value obtained from the two methods using the SQ80 module. The different methods produced different values of series resistance and from the plots, the effect of correctly

estimating the series resistance can be seen. It can also be noted that even at low irradiance the accuracy is maintained.

Table 3.5 Summary of graphs under varying irradiance

IRRADIANCE	**Method A**		**Method B**	
1 kW/m^2	Voc	I @ V=20	Voc	I @ V=20
Model 1	21.79534	2.77148	21.79381	2.88524
Model 2	21.79181	2.76704	21.79139	2.88223
Model 3	21.79181	2.76704	21.79363	2.884683
Model 4	21.79534	2.77148	21.79363	2.884683
Model 5	21.79534	2.77148	21.79363	2.884683
Measured	21.88	2.75	21.88	2.75
IRRADIANCE	**Method A**		**Method B**	
0.8 kW/m^2	Voc	I @ V=20	Voc	I @ V=20
Model 1	21.60401	2.22667	21.58055	2.258927
Model 2	21.60058	2.22277	21.57823	2.256272
Model 3	21.60369	2.22581	21.58038	2.258451
Model 4	21.60401	2.22667	21.58038	2.258451
Model 5	21.59883	2.22077	21.57462	2.251863
Measured	21.65	2.16	21.65	2.16
IRRADIANCE	**Method A**		**Method B**	
0.6 kW/m^2	Voc	I @ V=20	Voc	I @ V=20
Model 1	21.37035	1.62474	21.3248	1.589599
Model 2	21.36709	1.62142	21.32263	1.587297
Model 3	21.37006	1.62404	21.32464	1.589218
Model 4	21.37035	1.62474	21.32464	1.589218
Model 5	21.35909	1.61321	21.31234	1.576116
Measured	21.35	1.60	21.35	1.60
IRRADIANCE	**Method A**		**Method B**	
0.4 kW/m^2	Voc	I @ V=20	Voc	I @ V=20
Model 1	21.0772	0.96393	21.01241	0.877957
Model 2	21.07423	0.96118	21.01048	0.875997
Model 3	21.07695	0.96342	21.01229	0.877687
Model 4	21.0772	0.96393	21.01229	0.877687
Model 5	21.05879	0.94678	20.99259	0.857611
Measured	21.03	0.95	21.03	0.95
IRRADIANCE	**Method A**		**Method B**	
0.2 kW/m^2	Voc	I @ V=20	Voc	I @ V=20
Model 1	20.69795	0.24517	20.62332	0.125877
Model 2	20.69546	0.24298	20.62173	0.124239
Model 3	20.69779	0.24489	20.62324	0.125735
Model 4	20.69795	0.24517	20.62324	0.125735
Model 5	20.67083	0.22097	20.59488	0.096074
Measured	20.71	0.25	20.71	0.25

An analysis of the deviation of the simulated values from the measured values of open circuit voltage, Voc for all the different models under varying irradiance is shown in figure 3.12. The deviation is evaluated as the absolute value of the difference between the simulated values of open circuit voltage and the measured values of open circuit voltage for each model under varying irradiance, as shown in (3.70).

$$\text{Deviation} = |V_{oc(\text{measured})} - V_{oc(\text{simulated})}| \quad (3.70)$$

where $V_{oc(\text{simulated})}$ is the value of V_{oc} obtained from simulations and $V_{oc(\text{measured})}$ is the value of V_{oc} obtained from experimental measurements.

It can be seen from the graphs that for the varying irradiance values that estimation method A presents the lowest deviation of the simulated value of V_{oc} from the measured values.

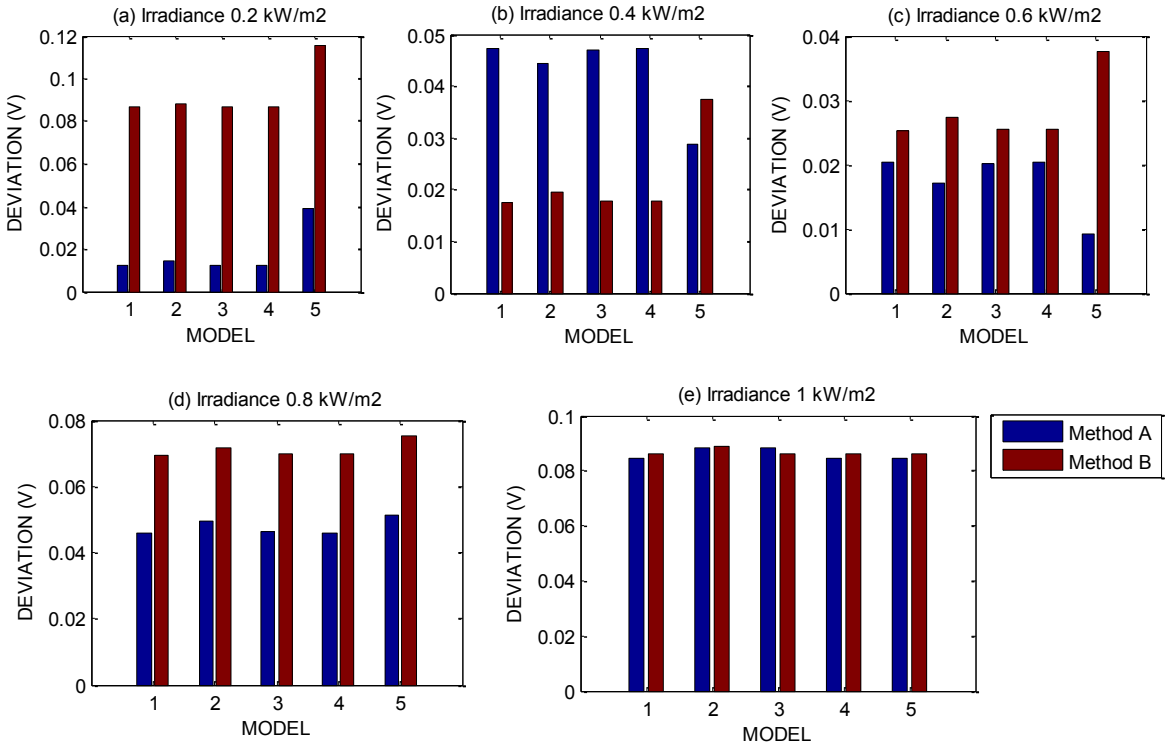

Figure 3.12 Bar graphs showing the deviation on simulation and measured values of V_{oc} for the different models under varying irradiance

Figure 3.13 and figure 3.14 show graphs plotted using KC200GT parameters using the two methods under varying irradiance. Figure 3.15 is an extract from the KC200GT module datasheet. The same can be observed from the graphs in figure 3.13 and figure 3.14 when comparing with the datasheet plot in figure 3.15.

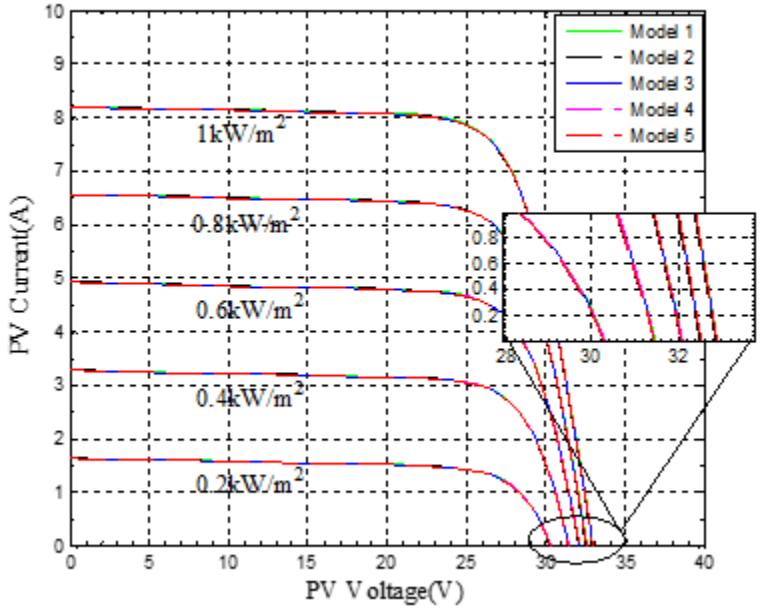

Figure 3.13 I-V Characteristic for KC200GT module under varying irradiance for models 1, 2, 3, 4 and 5, using parameter estimation method A.

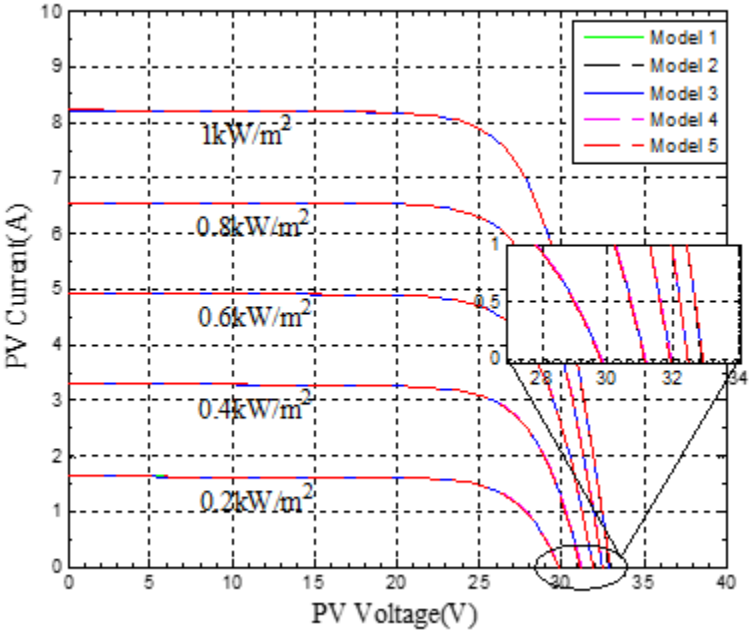

Figure 3.14 I-V Characteristic for KC200GT module under varying irradiance for models 1, 2, 3, 4 and 5, using parameter estimation method B.

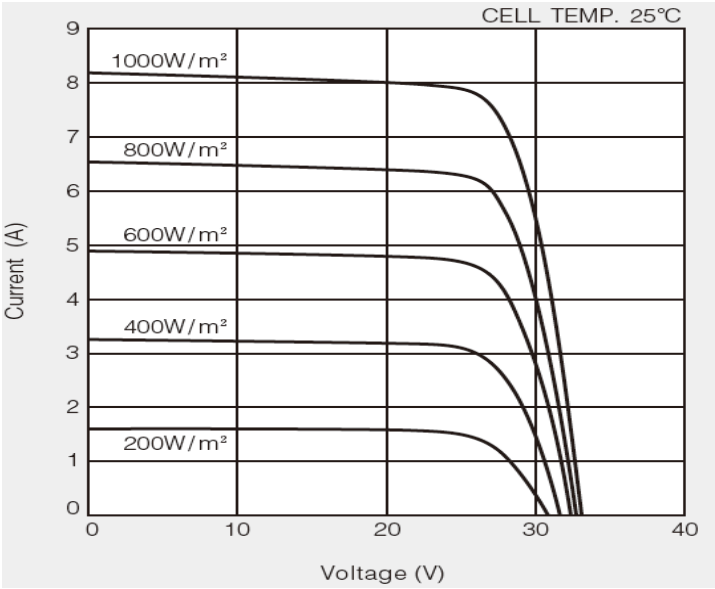

Figure 3.15 I-V Characteristic for KC200GT module under varying irradiance extracted from datasheet.

Figure 3.16 and figure 3.17 show I-V characteristic plots for the SQ80 simulated under varying temperature for all five models using method A and method B respectively and also includes graphs plotted using measured data for the SQ80 module. It can be seen that using method A, the results obtained are more comparable to the measured values than for the one using method B, considering the shape of the curves towards the open circuit voltage.

The same effect can be seen from figure 3.18 and figure 3.19, which depict the plots from panel KC200GT using the two methods under varying temperature, when compared with the datasheet extracted plots in figure 3.20.

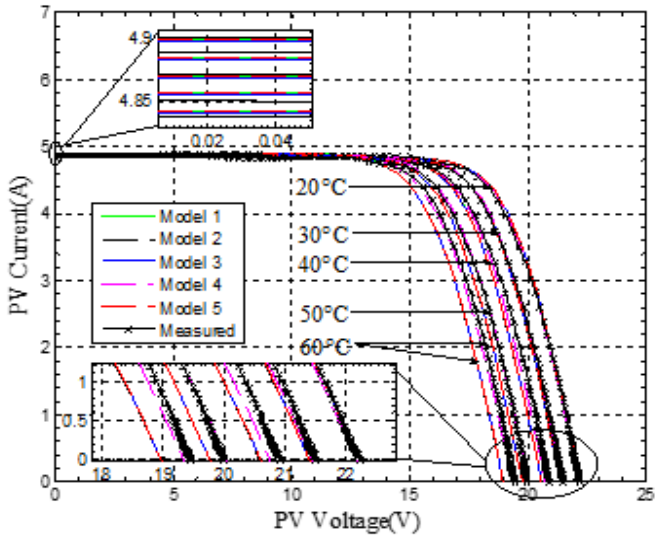

Figure 3.16 I-V Characteristic for SQ80 module under varying temperature for model 1, 2, 3, 4, 5 and measured values, using parameter estimation method A.

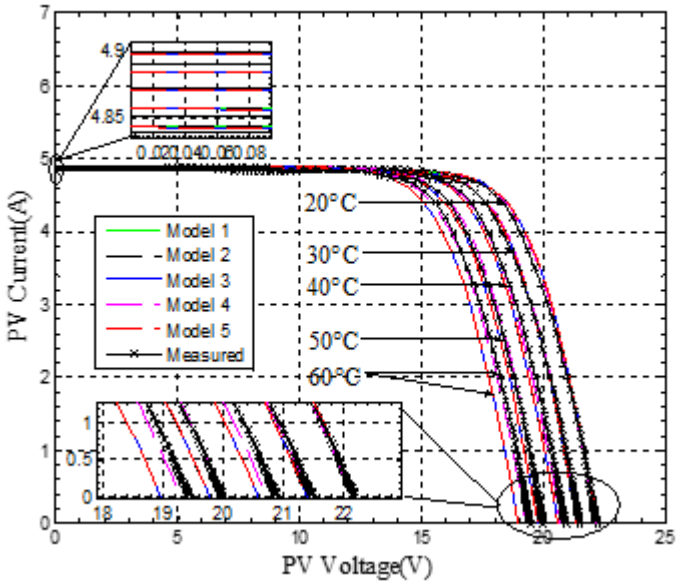

Figure 3.17 I-V Characteristic for SQ80 module under varying temperature for model 1, 2, 3, 4, 5 and measured values, using parameter estimation method B.

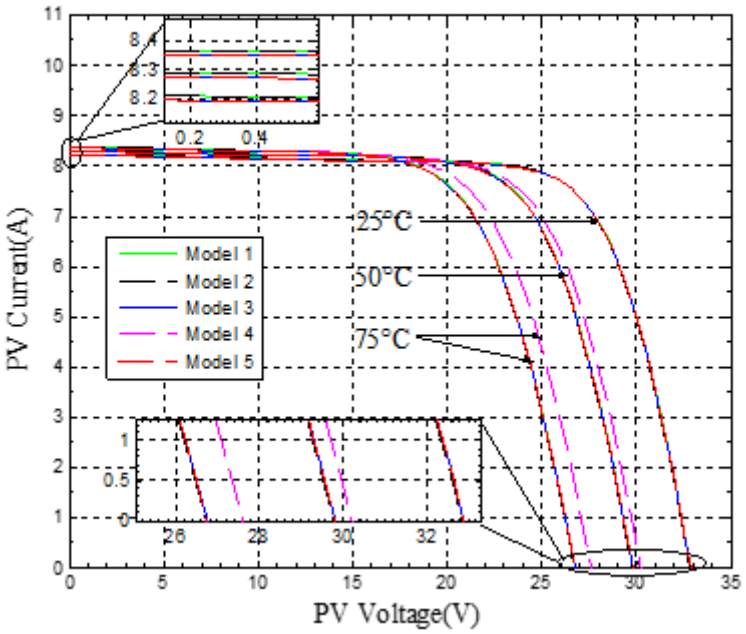

Figure 3.18 I-V Characteristic for KC200GT module under varying temperature for model 1, 2, 3, 4 and 5, using parameter estimation method A.

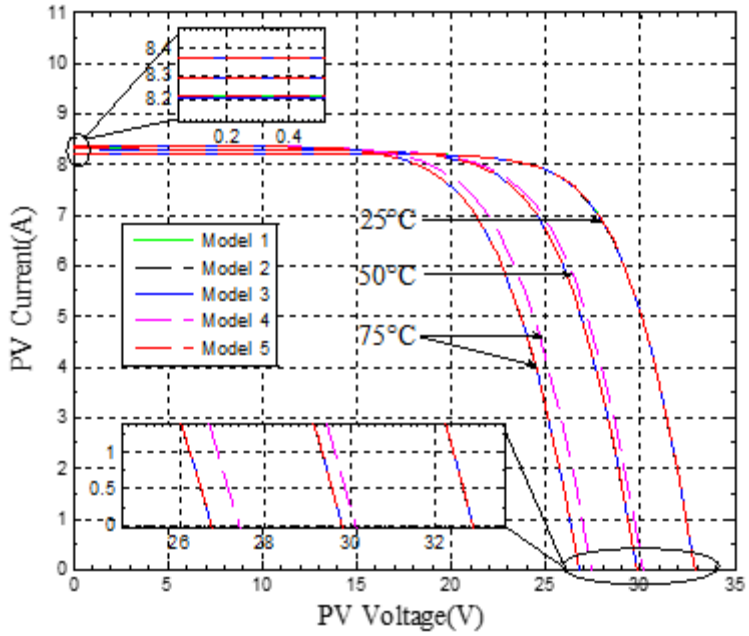

Figure 3.19 I-V Characteristic for KC200GT module under varying temperature for model 1, 2, 3, 4 and 5, using parameter estimation method B.

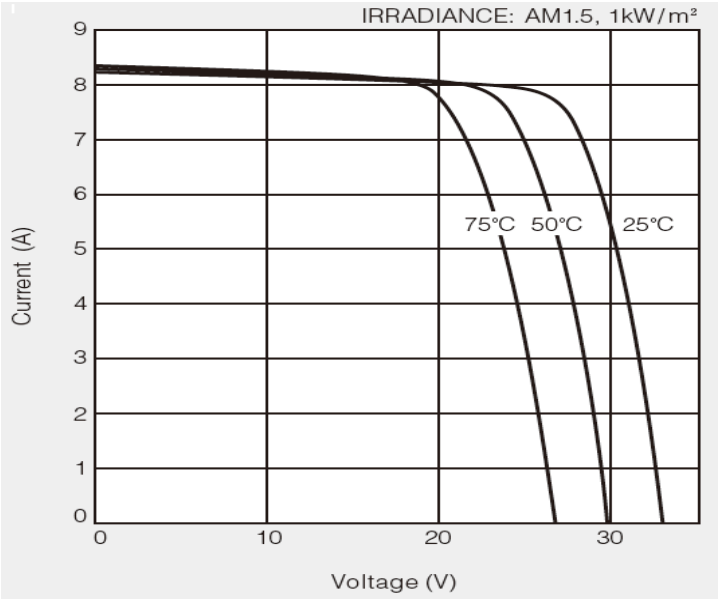

Figure 3.20 I-V Characteristic for KC200GT module under varying Temperature extracted from datasheet.

The open circuit voltage response to temperature variation from the different modelling methods as depicted in the plots show that at temperatures around the STC, the models depict similar behaviour. However as the temperature increases one of the plots tends to deviate from the other corresponding plots i.e. model 4 deviates from model 1, 2, 3 and 5.

It can be seen though that the graph that best approximates the plot using measured values with a small deviation is model 4. Table 3.6 gives a summary of the variation of the open circuit voltage and short circuit current for the different models and estimation methods under varying temperature for the SQ80 module. The effect on the short circuit current is the same for all methods and this basically shows that there is minimal dependence between short circuit current and changes in temperature. The effect of the difference in series resistance can be seen in the shape of the two graphs shown in figure 3.16 and figure 3.17, that the values produced from method A produces graphs which are more comparable to the plot with measured values.

Table 3.6 Summary of graphs under varying temperature

TEMP	**Method A**		**Method B**	
20°C	Voc	Isc	Voc	Isc
Model 1	22.20484	4.843	22.20479	4.843
Model 2	22.20136	4.84300	22.20242	4.843001
Model 3	22.20451	4.84119	22.2046	4.842109
Model 4	22.15290	4.84300	22.15788	4.842109
Model 5	22.20484	4.84300	22.20461	4.842109
Measured	22.20	4.839	22.20	4.839
TEMP	**Method A**		**Method B**	
30°C	Voc	Isc	Voc	Isc
Model 1	21.38991	4.85700	21.38825	4.857
Model 2	21.38632	4.85700	21.38576	4.856999
Model 3	21.38959	4.85518	21.38807	4.856106
Model 4	21.44186	4.85700	21.43454	4.856106
Model 5	21.38991	4.85700	21.38806	4.856106
Measured	21.50	4.851	21.50	4.851
TEMP	**Method A**		**Method B**	
40°C	Voc	Isc	Voc	Isc
Model 1	20.58050	4.871	20.57906	4.871
Model 2	20.57704	4.870992	20.57669	4.870996
Model 3	20.58023	4.869179	20.57891	4.870103
Model 4	20.73592	4.870992	20.71694	4.870103
Model 5	20.58050	4.870992	20.57887	4.870103
Measured	20.90	4.872	20.90	4.872
TEMP	**Method A**		**Method B**	
50°C	Voc	Isc	Voc	Isc
Model 1	19.77402	4.885	19.77372	4.885
Model 2	19.77043	4.884987	19.77121	4.884993
Model 3	19.77378	4.883173	19.77359	4.884101
Model 4	20.03502	4.884987	20.00486	4.884101
Model 5	19.77402	4.884987	19.77351	4.884101
Measured	20.00	4.890	20.00	4.890
TEMP	**Method A**		**Method B**	
60°C	Voc	Isc	Voc	Isc
Model 1	18.95958	4.899	18.9579	4.898999
Model 2	18.95616	4.898982	18.95553	4.89899
Model 3	18.9594	4.897168	18.95782	4.898098
Model 4	19.33915	4.898982	19.29812	4.898098
Model 5	18.95958	4.898982	18.95769	4.898098
Measured	19.45	4.900	19.45	4.900

An analysis of the deviation of the simulated values from the measured values of open circuit voltage, Voc for all the different models under varying temperature is shown in figure 3.21. The deviation is calculated using (3.70). It can be observed that as the temperature is increased, the deviation seen on model 4 values is the smallest when compared with the other models. Another point to note is that the deviation on method A is generally smaller than the deviation on method B.

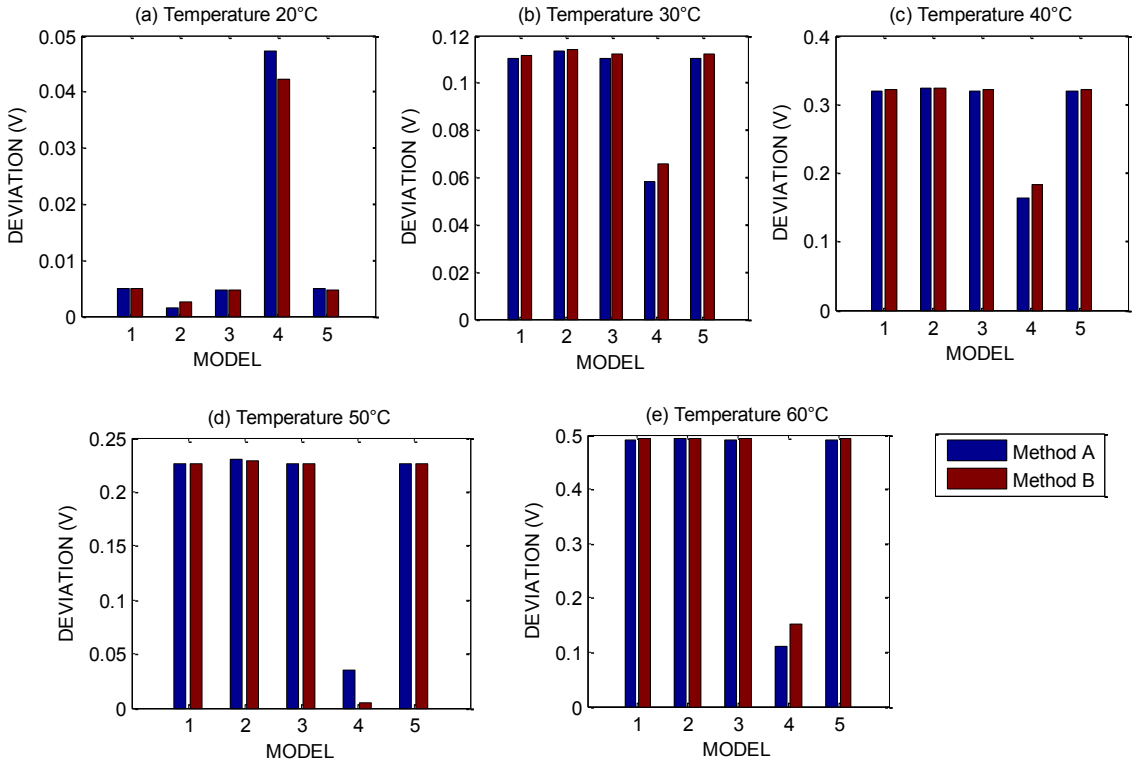

Figure 3.21 Bar graphs showing the deviation on simulation and measured values of V_{oc} for the different models under varying temperature

3.5 Conclusion

In this chapter, different modelling methods (equations) recommended by different authors in literature are described (detailed under section 3.12) and have been verified by simulation and experimental results. The modelling equations that best approximate the plots from measured values for the SQ80 PV model, which is also applicable to any PV module with datasheet parameters was recognized as shown by using a different module with different ratings from the SQ80 analysed. Model 4 is justified in this case. The study also involved detailing the parameter estimation methods used within the 5 models that were classified. The parameter estimation has been identified to have an effect on the shape of the curve as well as on the open circuit voltage response under varying irradiance as shown by the graphs. It can be concluded that the iterative method of extracting parameters, i.e. method A produced more comparable results. Therefore, as long as there is convergence, it can be concluded that the iteration techniques produce more accurate results for estimated parameters, so does the use of model 4 equations for non STC conditions.

4 Double-Diode model

In chapter 3, a comparative analysis of the different variants of the single-diode model were analysed. A combination of parameter estimation method and the most accurate modelling equations were selected based on the results that were obtained from simulations and manufacturer's datasheet.

In this chapter, the double-diode representation of a PV module is discussed. A new method for extracting parameters of a double-diode model is proposed and described. This method is based on the simplified double-diode representation of PV modules. Verification of the modelling method is done using different PV modules and comparing the graphs plotted by simulation for the proposed method against the graphs plotted by simulation for another existing double-diode modelling method for the various PV modules. Also, further comparison is done against graphs extracted from PV modules' datasheets. The proposed modelling method is also validated by comparing the simulation results with graphs plotted from experimentally measured data for the SQ80 PV module.

The derivation of the non-linear equations for the double-diode model is first discussed as well as the new parameter extraction algorithm in section 4.1. The extracted parameters are then used to plot the different graphs under varying conditions of temperature and irradiance in section 4.2. The results obtained are discussed in section 4.3 and the conclusion is outlined in section 4.4.

4.1 Parameter Estimation

Figure 4.1 shows the equivalent circuit for the double-diode representation of a solar cell. It consists of a current source, two diodes connected in parallel as well as the series and shunt resistances.

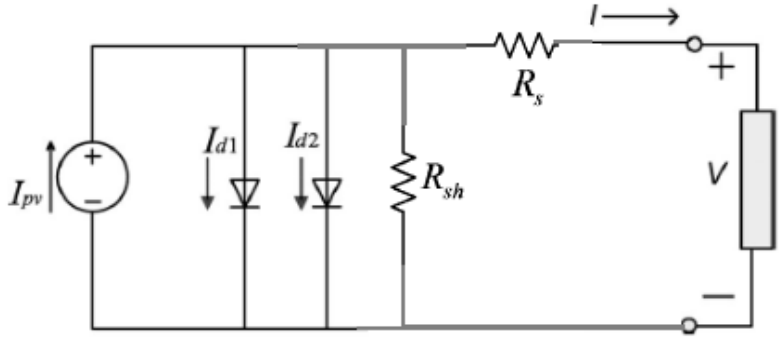

Figure 4.1 Equivalent circuit for double-diode model

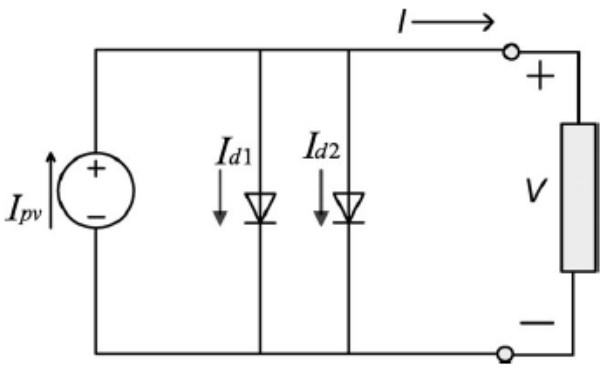

Figure 4.2 Equivalent circuit for simplified double-diode model

The simplified double-diode model is represented as shown in figure 4.2 [8]. The relationship between the current at the output of a PV module, consisting of a number of cells connected in series or parallel, and the voltage which appears across the output can be depicted by (4.1), which is found by summation of the currents according to Kirchhoff's Current Law:

$$I = I_{ph} - I_{01}\left[\exp\left(\frac{V}{A_1 V_T}\right) - 1\right] - I_{02}\left[\exp\left(\frac{V}{A_2 V_T}\right) - 1\right] \quad (4.1)$$

where I is the module current; V is the module voltage; I_{ph} is the photo generated current; I_{01} is the reverse saturation current due to diffusion of the charge carriers in the semiconductor, I_{02} is the reverse saturation current due to recombination in the space charge region, A_1 and A_2 is the ideality constant for diode 1 and 2 respectively; V_T is the junction thermal voltage and can be expressed as $V_T = \frac{N_s kT}{q}$, where N_s is the number of series connected cells in the module; k is the Boltzmann's constant equal to 1.38×10^{-23}; q is the electron charge equal to 1.602×10^{-19}; and T is the temperature. In (4.1) there are 5 parameters which are unknown, that is, I_{01}, I_{02}, A_1, A_2 and I_{ph}.

4.1.1 Derivation of Non-Linear equations

The three operating conditions of a PV module namely, short circuit, open circuit and maximum power point, are used to derive the equations which are used for the proposed parameter extraction method.

Under short circuit conditions, where $I = I_{sc}$ and $V = 0$, (4.1) is reduced to (4.2)

$$I_{ph} = I_{sc} \tag{4.2}$$

In open circuit operation, where $I = 0$ and $V = V_{oc}$,(4.1) becomes (4.3):

$$0 = I_{ph} - I_{01}\left[\exp\left(\frac{V_{oc}}{A_1 V_T}\right) - 1\right] - I_{02}\left[\exp\left(\frac{V_{oc}}{A_2 V_T}\right) - 1\right] \tag{4.3}$$

At maximum power point operation, where $I = I_{mp}$ and $V = V_{mp}$, (4.1) becomes (4.4):

$$I_{mp} = I_{ph} - I_{01}\left[\exp\left(\frac{V_{mp}}{A_1 V_T}\right) - 1\right] - I_{02}\left[\exp\left(\frac{V_{mp}}{A_2 V_T}\right) - 1\right] \tag{4.4}$$

Substituting (4.2) in (4.3) and (4.4) results in the system of equations (4.5) and (4.6).

$$I_{01}\left[\exp\left(\frac{V_{oc}}{A_1 V_T}\right) - 1\right] + I_{02}\left[\exp\left(\frac{V_{oc}}{A_2 V_T}\right) - 1\right] = I_{sc} \tag{4.5}$$

$$I_{01}\left[\exp\left(\frac{V_{mp}}{A_1 V_T}\right) - 1\right] + I_{02}\left[\exp\left(\frac{V_{mp}}{A_2 V_T}\right) - 1\right] = I_{sc} - I_{mp} \tag{4.6}$$

The next step is to solve the two equations, (4.5) and (4.6) to find expressions for I_{01} and I_{02}. In solving the two equations we make the assumptions that $\left(\frac{V_{oc}}{A_1 V_T}\right) \gg 1$, $\exp\left(\frac{V_{oc}}{A_2 V_T}\right) \gg 1$, $\exp\left(\frac{V_{mp}}{A_1 V_T}\right) \gg 1$ and $\exp\left(\frac{V_{mp}}{A_2 V_T}\right) \gg 1$ as per [34], which reduces (4.5) and (4.6) to (4.7) and (4.8) :

$$I_{01}\exp\left(\frac{V_{oc}}{A_1 V_T}\right) + I_{02}\exp\left(\frac{V_{oc}}{A_2 V_T}\right) = I_{sc} \tag{4.7}$$

$$I_{01}\exp\left(\frac{V_{mp}}{A_1 V_T}\right) + I_{02}\exp\left(\frac{V_{mp}}{A_2 V_T}\right) = I_{sc} - I_{mp} \tag{4.8}$$

Rearranging (4.7) so that it is written in terms of I_{01}, we get (4.9):

$$I_{01} = \frac{I_{sc} - I_{02}\exp\left(\frac{V_{oc}}{A_2 V_T}\right)}{\exp\left(\frac{V_{oc}}{A_1 V_T}\right)} \tag{4.9}$$

Substituting (4.9) in (4.8) and rearranging, making I_{02} the subject of the expression we get (4.10)

$$I_{02} = \frac{(I_{sc}-I_{mp})\exp\left(\frac{V_{oc}}{A_1 V_T}\right)-I_{sc}\exp\left(\frac{V_{mp}}{A_1 V_T}\right)}{\exp\left(\frac{V_{oc}}{A_2 V_T}\right)\exp\left(\frac{V_{mp}}{A_1 V_T}\right)+\exp\left(\frac{V_{oc}}{A_1 V_T}\right)\exp\left(\frac{V_{mp}}{A_2 V_T}\right)} \tag{4.10}$$

Then finally we substitute (4.10) in (4.9) to get (4.11):

$$I_{01} = \frac{I_{sc}}{\exp\left(\frac{V_{oc}}{A_1 V_T}\right)} - \frac{\left[(I_{sc}-I_{mp})\exp\left(\frac{V_{oc}}{A_1 V_T}\right)-I_{sc}\exp\left(\frac{V_{mp}}{A_1 V_T}\right)\right]\exp\left[\frac{V_{oc}}{V_T}\left(\frac{1}{A_2}-\frac{1}{A_1}\right)\right]}{\exp\left(\frac{V_{oc}}{A_2 V_T}\right)\exp\left(\frac{V_{mp}}{A_1 V_T}\right)+\exp\left(\frac{V_{oc}}{A_1 V_T}\right)\exp\left(\frac{V_{mp}}{A_2 V_T}\right)} \tag{4.11}$$

We now have three equations (4.3), (4.10) and (4.11) which will be used to extract the parameters. The next section describes how the values of A_1 and A_2 are found.

4.1.2 Parameter extraction Algorithm

In section 4.1.1, three equations were derived which can be used in extracting of the STC parameters. There are however 5 unknown parameters to be extracted which means that the three equations cannot be solved to obtain the 5 unknown parameters.

A different way of estimating the ideality factors A_1 and A_2 is proposed. It involves adjusting of the values such that a pair of ideality factors is obtained which will produce a value of maximum power which closely matches the one on the PV module's datasheet at the same time ensuring that the values of the two reverse saturation currents I_{01} and I_{02} are both positive.

A detailed analysis of the effect, the two ideality factors have on the maximum power point of the I-V characteristics was done and the following observations were made:

1. The solution $A_1 = A_2$ does not exist for any value of A_1 or A_2 in any PV module, unlike what was assumed in [40] and [41].
2. The value of $A_2 > A_1$ for positive values of reverse saturation currents.
3. There is a minimum value of A_2 for every PV module where the equations will produce both positive values of reverse saturation current.

Figure 4.3, figure 4.4, figure 4.5, figure 4.6, figure 4.7 and figure 4.8 show graphical representations of this behaviour for five PV modules, GEPV110, JC260S, MSX-60, SQ80, KC200GT and U-EA120 of different technologies and ratings whose details are provided in table 4.1.

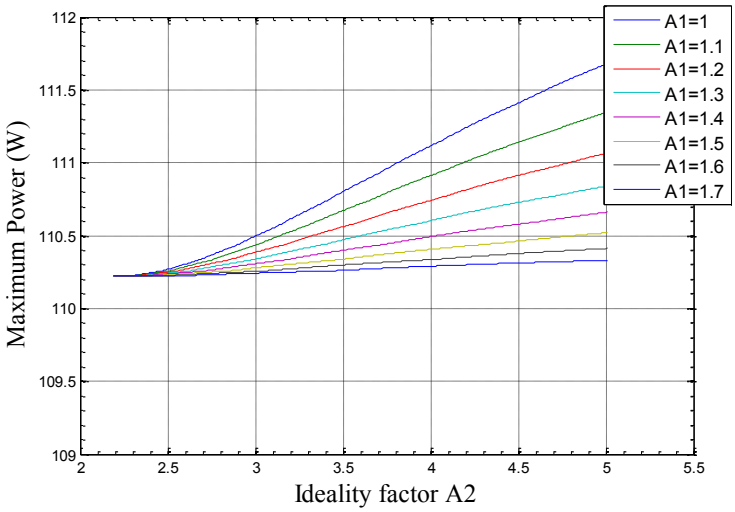

Figure 4.3 Variation of maximum power with ideality factors $\mathbf{A_1}$ and $\mathbf{A_2}$ for GEPV110 module

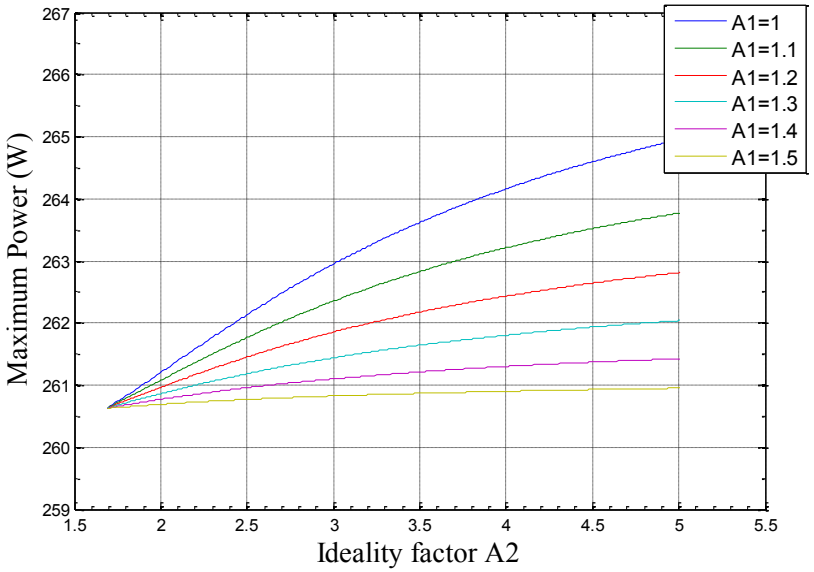

Figure 4.4 Variation of maximum power with ideality factors $\mathbf{A_1}$ and $\mathbf{A_2}$ for JC260S module

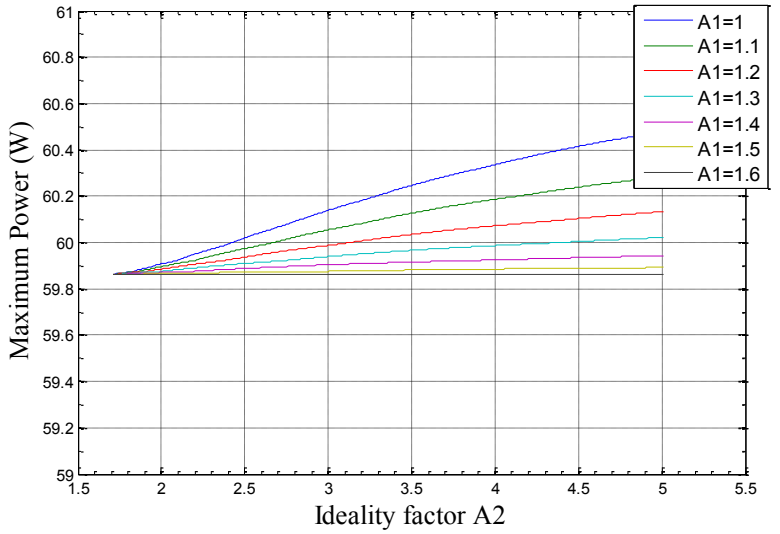

Figure 4.5 Variation of maximum power with ideality factors $\mathbf{A_1}$ and $\mathbf{A_2}$ for MSX-60 module

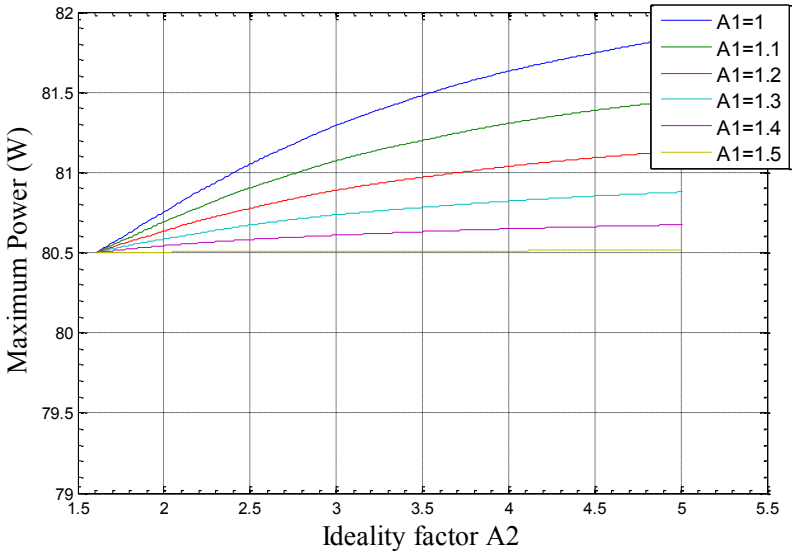

Figure 4.6 Variation of maximum power with ideality factors $\mathbf{A_1}$ and $\mathbf{A_2}$ for SQ80 module

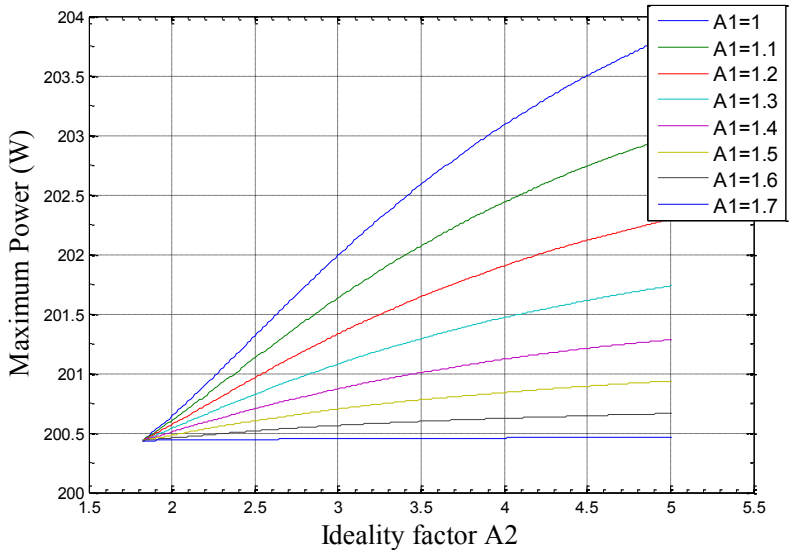

Figure 4.7 Variation of maximum power with ideality factors $\mathbf{A_1}$ and $\mathbf{A_2}$ for KC200GT module

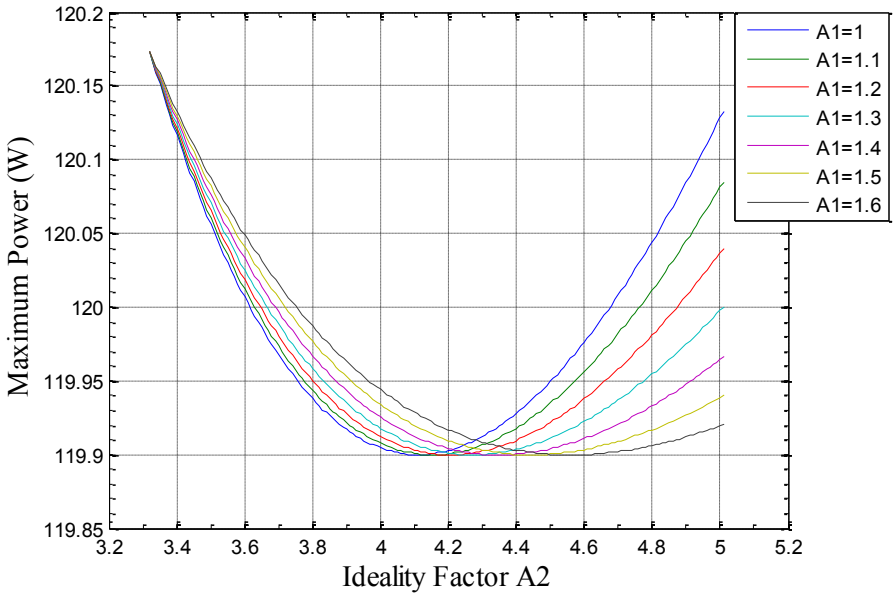

Figure 4.8 Variation of maximum power with ideality factors $\mathbf{A_1}$ and $\mathbf{A_2}$ for UEA120 module

Based on the above mentioned analysis, an algorithm was derived (see figure 4.9), which is able to determine the correct pair of values A_1 and A_2 which will ensure that the maximum power calculated using this model will be the closest estimation to the value extracted from the datasheet and at the same time ensuring that positive values

of reverse saturation currents are obtained for both diodes. The algorithm also caters for the different behaviour of the thin film PV module U-EA120 as depicted in figure 4.8 by finding the minimum value of maximum power closest to the maximum power value in the datasheet. Table 4.1 shows the STC parameters for the six PV modules analysed in this work extracted from the datasheets for the SQ80 [44], KC200GT [45], MSX-60 [46], JC260S [47], GEPV110 [48] and U-EA120 [49] PV modules.

Table 4.1 Data sheet parameters

Parameter	**SQ80**	**KC200GT**	**MSX-60**	**JC260S**	**GEPV110**	**U-EA120**
Crystalline Technology	**Mono**	**Poly**	**Poly**	**Mono**	**Mono**	**Thin Film**
N_s	36	54	36	60	36	106
I_{sc}	4.85A	8.21A	3.8	9.1	7.4A	2.8A
V_{oc}	21.8V	32.9V	21.1	37.7	21.2V	71V
V_{mp}	17.5V	26.3V	17.1	30.4	16.7V	55V
I_{mp}	4.58A	7.61A	3.5	8.55	6.6A	2.18
P_{mp}	80.15	200.1430	59.85	259.92	110.22	119.9
K_I(A/°C)	0.0014	0.00318	0.003	0.0003	0.003	0.00056
K_V(V/°C)	-0.081	-0.123	-0.08	-0.310	-0.08	-0.0039

Figure 4.9 shows a flow chart which depicts the steps followed in implementation of this algorithm. Separate steps are followed and implemented in Matlab for finding P_{max} as well as the minimum value of A_2 as shown in figure 4.10 and figure 4.11. P_{max}

is the maximum power calculated for a particular combination of values of ideality factors A_1 and A_2.

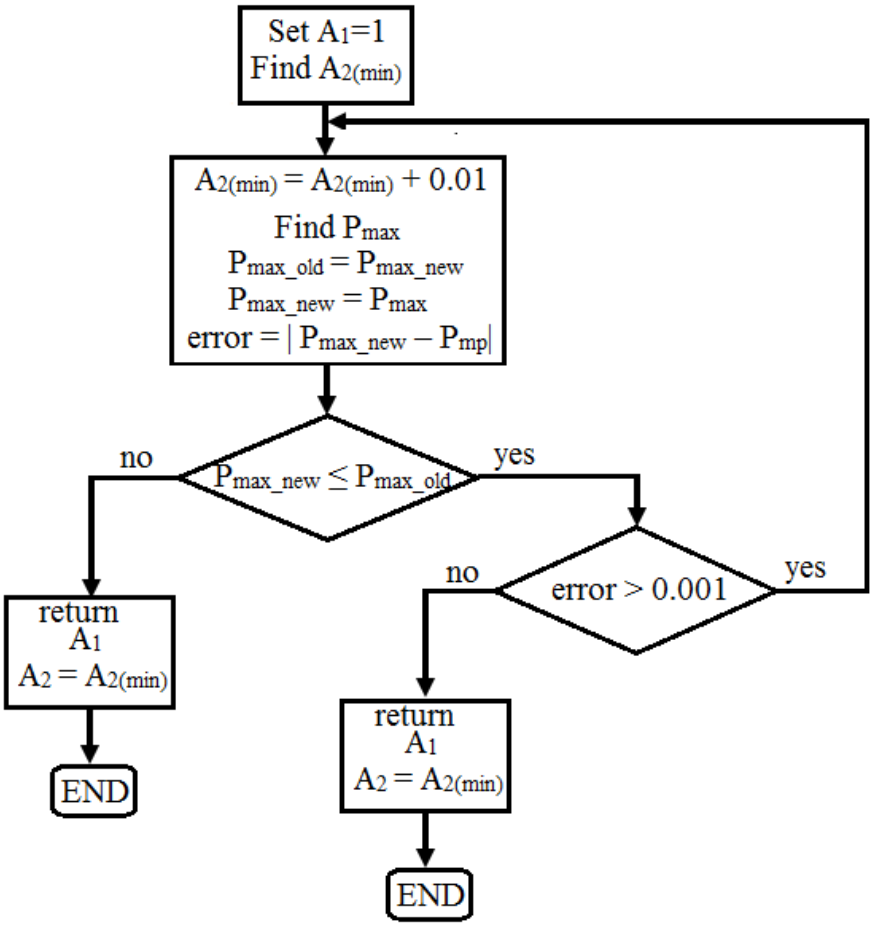

Figure 4.9 Algorithm for estimation of ideality factors $\mathbf{A_1}$ and $\mathbf{A_2}$

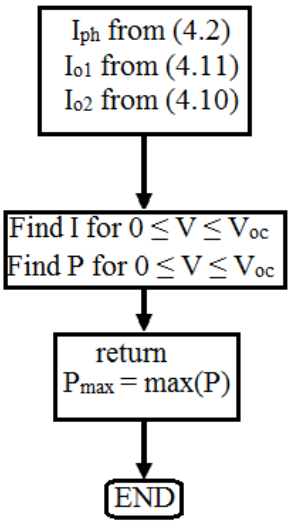

Figure 4.10 Steps for finding the maximum power, $\mathbf{P_{max}}$

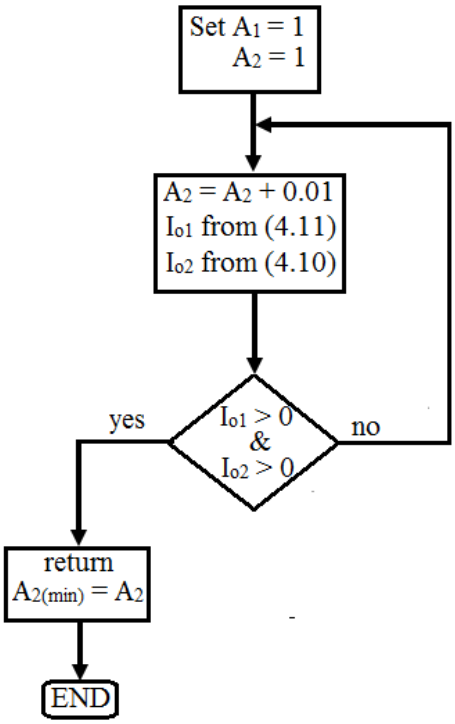

Figure 4.11 Steps for finding the value of $\mathbf{A_{2(min)}}$

In summary: to get A_2, we set $A_1 = 1$ (using an ideal value for A_1 is justified later) and then increment A_2 in steps of 0.01, at each step evaluating I_{02} and I_{01} using (4.10) and (4.11) until we get to the correct value of $A_{2(\min)}$. Also for P_{max} we evaluate the current as well as power for values of voltage ranging from 0 to V_{oc} using (4.1), (4.2), (4.10) and (4.11), and then taking P_{max} as the maximum calculated value of power. A matlab code was written to implement this algorithm shown in appendix A4 for the six selected PV modules and the results are summarized in table 4.2.

Table 4.2 STC parameters extracted using algorithm

Parameter	**Estimated value**					
	SQ80	**KC200GT**	**MSX-60**	**JC260S**	**GEPV110**	**U-EA120**
I_{o1}(A)	6.37×10^{-13}	1.6×10^{-12}	6.182×10^{-12}	1.316×10^{-12}	1.242×10^{-11}	3.0721×10^{-12}
I_{o2}(A)	2.135×10^{-6}	1.804×10^{-5}	6.061×10^{-6}	4.723×10^{-6}	2.1857×10^{-4}	2.1×10^{-3}
I_{ph}(A)	4.85	8.21	3.8	9.1	7.4	2.6
A_1	1	1	1	1	1	1
A_2	1.61	1.82	1.71	1.69	2.2	3.8
P_{max}(W)	80.5003	200.4347	59.8619	260.6297	110.22	120.0224
P_{mp}(W)	80.15	200.1430	59.85	259.92	110.22	119.9
$P_{\max error}$%	0.4371	0.1457	0.0198	0.2731	0	0.1021

4.2 Dependence on Temperature and Irradiance

As mentioned in previous sections, the second step in modelling is to use the parameters estimated under STC to evaluate the I-V characteristics of the PV module under varying temperature and irradiance conditions.

Parameters which are known to vary with changing temperature are the reverse saturation currents I_{01} and I_{02} which are strongly dependent on temperature as given in (4.12) and (4.13) [34]:

$$I_{o1} = I_{o1,STC}\left[\frac{T}{T_{STC}}\right]^3 \exp\left(\frac{q}{A_1 k}\left(\frac{E_{g,STC}}{T_{STC}} - \frac{E_g}{T}\right)\right) \tag{4.12}$$

$$I_{o2} = I_{o2,STC}\left[\frac{T}{T_{STC}}\right]^{\frac{5}{2}} \exp\left(\frac{q}{2A_2 k}\left(\frac{E_{g,STC}}{T_{STC}} - \frac{E_g}{T}\right)\right) \tag{4.13}$$

where, T is the temperature of the module and , T_{STC} is the temperature at STC which is equal to 298K, E_g is the band gap energy at temperature T and $E_{g,STC}$ is the band gap energy at STC temperature. The equation (3.36) is used to calculate the band gap energy and is restated in this chapter as (4.14) [7].

$$E_g = E_{go} - \frac{\gamma T^2}{\beta + T} \tag{4.14}$$

where E_{go}, γ and β are fitting parameters as outlined in table 3.1.

Another parameter to be considered is the photo-generated current which is known to vary with both temperature and irradiance using (4.15) below [34]:

$$I_{ph} = (I_{ph,STC} + K_I \Delta T)G \tag{4.15}$$

where T is the temperature of the module, ΔT is the temperature difference $T - T_{STC}$, T_{STC} is the temperature at STC which is equal to 298K, $I_{ph,STC}$ is the photo-generated current estimated under STC and G is the ratio of the irradiance with respect to STC value, i.e. $1kW/m^2$.

In using the simplified double-diode model represented in (4.1), it was discovered that

the ideality factors have an effect on the open circuit voltage obtained under non-STC conditions. In varying the G from 1 to 0.2, the open circuit voltage obtained from the I-V characteristics tends to decrease and as a result deviate from the expected values. It can also be mentioned that as the temperature is increased, the open circuit voltage is reduced, but if ideality factor A_1 is increased from the ideal value, $A_1 = 1$, the value obtained for the open circuit voltage is decreased and as such causing a deviation from the expected values.

Based on the above mentioned observations, a correction factor on the diode ideality factor A_2 was derived, considering the logarithmic effects the reduced irradiance has on the open circuit voltage V_{oc}. As stated in [6], provided the module temperature is constant, the open circuit voltage values scale logarithmically with short circuit current which in turn shows a linear dependence on solar irradiance, meaning that the open circuit voltage has a logarithmic dependence on solar irradiance. At high irradiance, the open circuit V_{oc} is reduced by a small amount and at low irradiance the effect on the open circuit voltage is more significant, as a result a parameter α is derived and curve fitting is used to derive it. For instance, when $G = 0.8$, the value of V_{oc} obtained without the correction factor is less than the one on the datasheet, but after multiplying the ideality factor A_2 by 1.01 the value of V_{oc} obtained matches the one estimated from the datasheet. There is a logarithmic relationship between G and the number by which the ideality factor A_2 is multiplied. For $G = 0.8$, α can be calculated from $0.8 = \alpha^{0.01}$, from which $\alpha=2.037\times10^{-10}$. It follows that for every value of G, the ideality factor A_2 has to be multiplied by the correction factor $1 + \frac{\ln(G)}{\ln(\alpha)}$ to obtain the correct value of V_{oc}. The correction factor is dependent on G.

It can also be shown that increasing the ideality factor A_1, causes a reduction in V_{oc} as the temperature is increased, however an accurate value of V_{oc} is obtained by using $A_1 = 1$, as such the first diode is considered ideal as shown in table 4.2.

Consequently, (4.1) can be rewritten as (4.16)

$$I = I_{ph} - I_{01}\left[\exp\left(\frac{V}{V_{t1}}\right) - 1\right] - I_{02}\left[\exp\left(\frac{V}{V_{t2}}\right) - 1\right] \quad (4.16)$$

where $V_{t1}=A_1V_T$ and $V_{t2}=A_2V_T(1+\frac{\ln(G)}{\ln(\alpha)})$, $\alpha=2.037\times10^{-10}$.

4.3 Simulations

This section describes the simulations which were done to implement the method proposed in this study. Matlab/Simulink was used to simulate and plot the I-V characteristic graphs based on the proposed model. Figure A.3 (in Appendix) shows the different Simulink blocks used. The block labelled "PARAMETER ESTIMATION" is embedded with the Matlab function code for extraction of the five unknown parameters of the proposed double-diode model which is listed in appendix D. The other simulink function blocks shown in figure A.3 are summarized below.

Figure 4.12 shows the Matlab Simulink function block used to represent the equations for the proposed model as well as the Matlab function code embedded in the Simulink block. The function takes the STC values for A_1, A_2, I_{phn}, I_{o1n}, I_{o2n} and K_I as inputs, I_{o1n} and I_{o2n} are the STC values for the reverse saturation currents for diode 1 and diode 2 respectively, I_{phn} is the STC value for the photo-generated current. It also takes N_s as well as T and G. The outputs of the function are I_{o1}, I_{o2}, I_{ph}, V_{t1} and V_{t2}, which are parameters dependent on the temperature T and irradiance G. I_{o1} is calculated using (4.12), I_{o2} using (4.13) and I_{ph} is calculated using (4.15).

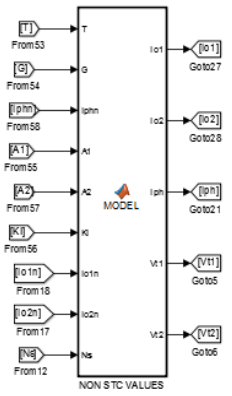


```
function [Io1, Io2,Iph, Vt1, Vt2] = MODEL( T, G, Iphn, A1, A2, Ki, Io1n,Io2n, Ns)
%Function evaluates the output parameters Io1,Io2,Iph,Vt1 and Vt2 at a specific
%temperature and irradiance.
q=1.602e-19;    % assign electron charge
K=1.38e-23;     % assign Boltzman's constant
Ego=1.166;      % assign fitting parameter for silicon
B=636;          % assign fitting parameter for silicon
M=4.7e-4;       % assign fitting parameter for silicon

Alpha=2.037e-10; % assign ideality factor correction factor

Vt1=K*298*A2*Ns/q;
Vt2=K*298*A2*(1+(log(G)/log(Alpha)))*Ns/q;

Eg=Ego-((M*T^2)/(T+B));  % calculate Eg(T)
Egn=Ego-((M*298^2)/(298+B)); % calculate band gap at STC

Iph=(Iphn+Ki*(T-298))*G; % calculate Iph with dependence on irradiance and temperature
Io1 = Io1n*((T/298)^3)*exp((q/(A1*K))*((Egn/298)-(Eg/T))); % calculate reverse saturation current for diode 1
Io2 = Io2n*((T/298)^(5/2))*exp((q/(2*A2*K))*((Egn/298)-(Eg/T))); % calculate reverse saturation current for diode 2

end
```

Figure 4.12 Simulink function block and Matlab code for calculation of non STC parameters of proposed model

Figure 4.13 shows the Simulink block which evaluates the PV module's current for values of V ranging from zero to V_{oc}. The input voltage is shown as a ramp input into

the Simulink block. The function takes the inputs as indicated and gives an output current using the PV current equation (4.1).

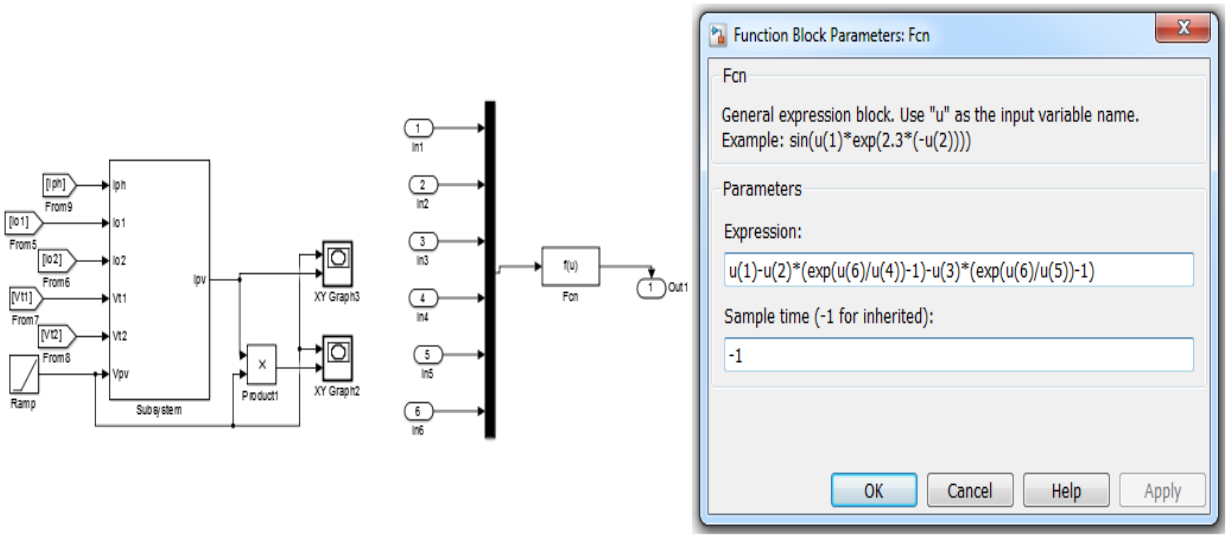

Figure 4.13 Simulink block for calculation of PV output current for proposed double-diode model

The Simulink blocks labelled KC200GT, SQ80, JC260S, MSX-60, GEPV110 and U-EA120 represent the STC parameters extracted from the datasheets of the respective PV modules.

4.4 Results and Discussion

Figure 4.10 outlines the steps followed in the calculation of maximum power. It requires values of the photo-generated current I_{ph} as well as the reverse saturation currents I_{o1} and I_{o2}. Table 4.3 shows the values of maximum power at STC calculated using the values of I_{ph}, I_{o1} and I_{o2}obtained in [8] and [34], and using the proposed model for the different PV modules KC200GT, MSX-60, JC260S and GEPV110 analysed in this study. Table 4.4 shows the % error calculated using (4.17) for the values obtained in table 4.3 with the respective maximum power obtained from the datasheet for the different PV modules.

$$\%\text{error} = \frac{|P_{mp(model)} - P_{mp(datasheet)}|}{P_{mp(datasheet)}} \tag{4.17}$$

where $P_{mp(model)}$ is the maximum power calculated using the proposed model, results

in [8] and results in [34], $P_{mp(datasheet)}$ is the maximum power given in the datasheets of the respective PV modules as shown in table 4.4.

As it can be seen, the values show that the model proposed in this paper has the lowest error which shows the high level of accuracy in relation to the manufacturer's datasheet parameters for maximum power at STC when compared with the %error calculated using results in [8] and [34].

A combination of (4.2), (4.12), (4.13), (4.15), (4.16) and the values of A_1 and A_2 estimated under STC are used to plot the I-V characteristics for three of the different PV modules considered in this work, the GEPV110, KC200GT and the SQ80 PV modules.

Table 4.3 Maximum power point values calculated at STC

	KC200GT	**MSX-60**	**JC260S**	**GEPV110**
Results in [8]	129.2516	60.1466	241.8529	-
Results in [34]	218.7518	-	-	119.663
This Model	200.4394	59.8632	260.6335	110.2207
Datasheet	200.143	59.85	259.92	110.22

Table 4.4 Maximum power point error values calculated at STC

	KC200GT	**MSX-60**	**JC260S**	**GEPV110**
Results in [8]	35.4204	0.4955	12.5749	-
Results in [34]	9.298	-	-	8.5674
This Model	0.1481	0.022	5.7861	0.0006

Figure 4.14 and figure 4.15 show the I-V characteristic plots for the GEPV110 PV module plotted using simulation values as well as an extract from the module's datasheet respectively. Table 4.5 shows the values of V_{oc} obtained by using the results in [34] as well as the ones obtained by using this method and those extracted from the datasheet for the GEPV110 PV module. Again it can be seen that the graph obtained from this method closely resembles the one on the manufacturer's datasheet. The same comparison was made using the plots for the KC200GT module as shown in figure 4.16 and figure 4.17 for varying irradiance and figure 4.18 and figure 4.19 for varying temperature. Table 4.6 shows the values of V_{oc} obtained by using the results in [34] as well as the ones obtained by using this method and those extracted from the datasheet for the KC200GT PV module for varying irradiance and temperature.

Based on the maximum power point error values calculated and listed in table 4.4, it can be concluded that the method proposed in this thesis is more accurate when compared with results obtained in [8] and [34]. It can further be noted that the values of V_{oc} obtained using the proposed method are comparable with the values extracted from the PV module's datasheets.

Table 4.5 Summary of graph for GEPV110 PV module

	V_{oc}		
	This Work	**Results in [34]**	**Estimate from Datasheet**
G=1kW/m^2 T=25°C	21.19	21.19	21.20
G=0.8kW/m^2 T=45°C	19.16	19.4	19.20
G=1kW/m^2 T=60°C	18.12	18.5	18.15

Table 4.6 Summary of graph for KC200GT PV module

IRRADIANCE		V_{oc}	
	This Work	**Results in [34]**	**Estimate from Datasheet**
1 kW/m^2	32.89	32.85	32.9
0.8 kW/m^2	32.6	32.52	32.7
0.6 kW/m^2	32.29	32.1	32.4
0.4 kW/m^2	31.8	31.48	31.7
0.2 kW/m^2	30.85	30.4	30.75
TEMPERATURE			
25°C	32.9	32.9	32.9
50°C	29.9	29.9	30.0
75°C	27.0	26.78	26.3

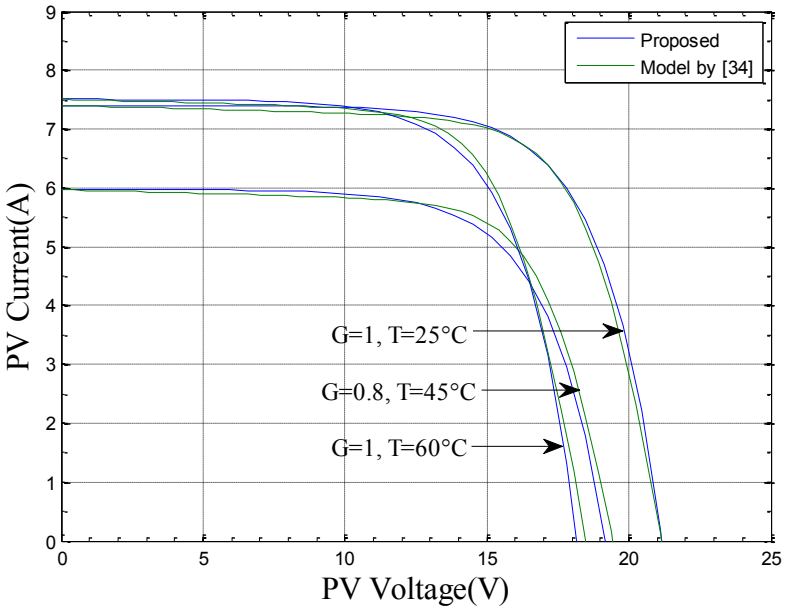

Figure 4.14 I-V Characteristics for GEPV110 PV module simulated from this work and using results from modelling by [34]

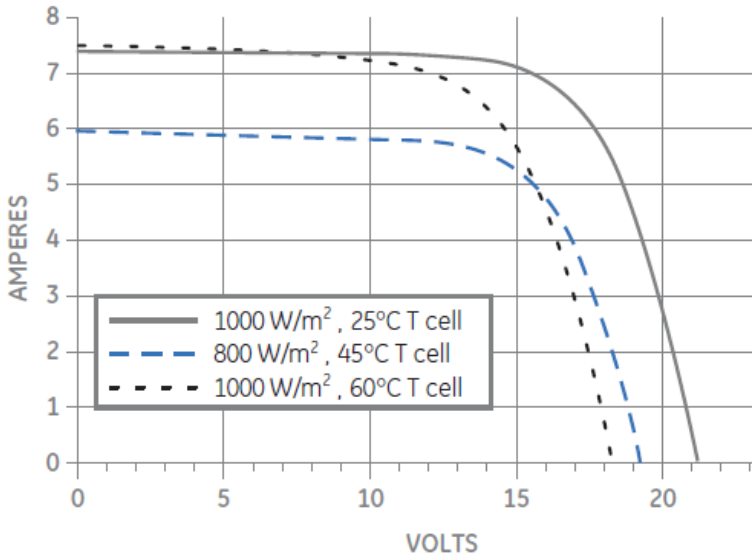

Figure 4.15 I-V characteristics for GEPV110 extracted from datasheet

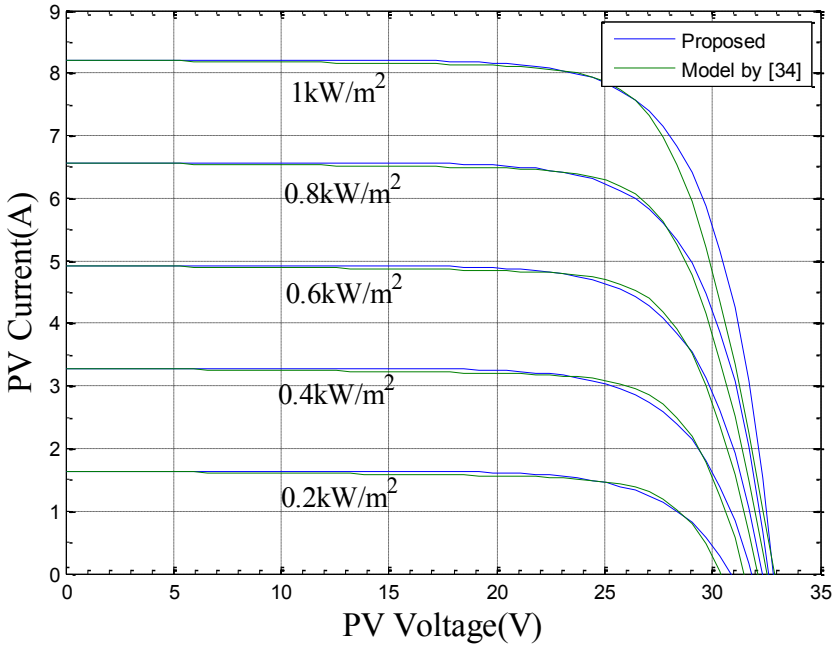

Figure 4.16 I-V characteristics for KC200GT PV module simulated using this work and using results from modelling by [34] under varying irradiance

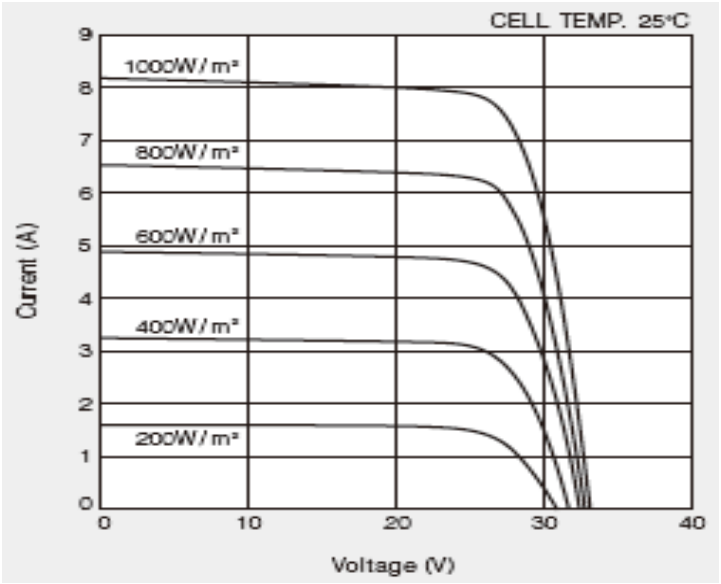

Figure 4.17 I-V characteristics for KC200GT PV module under varying irradiance extracted from datasheet.

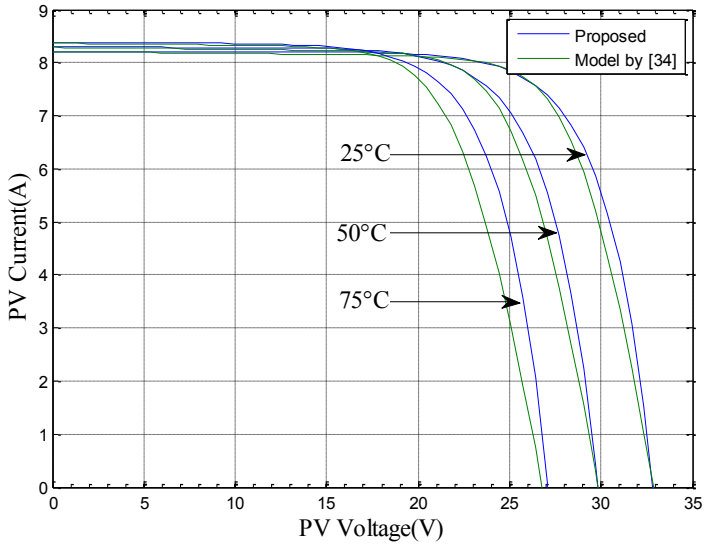

Figure 4.18 I-V Characteristics for KC200GT PV module simulated using this work and using results from modelling by [34] under varying temperature

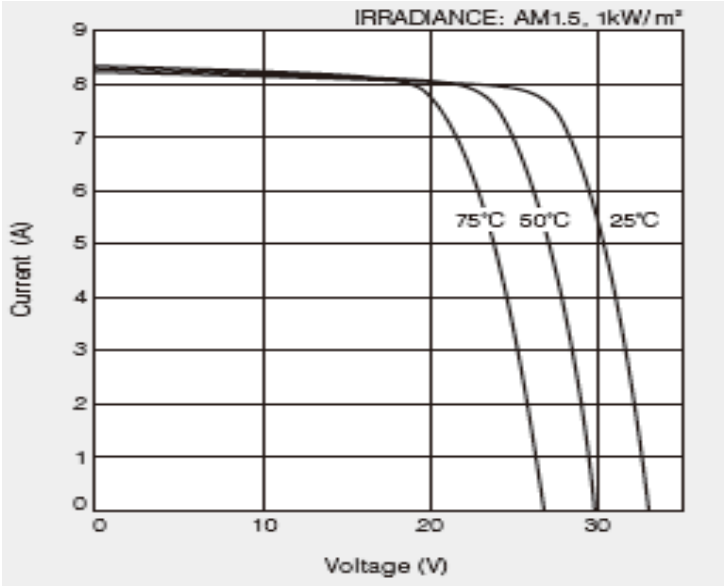

Figure 4.19 I-V characteristics for KC200GT PV module under varying temperature extracted from datasheet.

4.5 Experimental Validation of Model

In the previous section the simulation results were discussed and from the results, it is confirmed that the proposed double- diode model is much more accurate in modelling the various PV modules, therefore, experimental results shown in appendix E are used

to further validate the simulated results. figure 4.17 and figure 4.18 show the I-V characteristic plots for the SQ80 PV module obtained from simulations using the method proposed in this paper as well as experimentally measured values under varying irradiance and under varying temperatures respectively. Table 4.7 shows values of V_{oc} obtained from experimental values as well as from simulations using the proposed method. It can also be observed that the values obtained from simulations are comparable to the values obtained from experimental measurements especially near the V_{oc} region.

Table 4.7 Summary of graph for SQ80 PV module

IRRADIANCE	Voc		
	Simulation	**Experimental**	**Deviation**
1 kW/m^2	21.78	21.88	0.10
0.8 kW/m^2	21.64	21.65	0.01
0.6 kW/m^2	21.36	21.35	0.01
0.4 kW/m^2	21.05	21.03	0.02
0.2 kW/m^2	20.74	20.71	0.03
TEMPERATURE			
20°C	22.18	22.20	0.02
30°C	21.55	21.50	0.05
40°C	20.83	20.90	0.07
50°C	20.00	20.00	0.00
60°C	19.30	19.45	0.15

It is worth noting however that in other regions along the graphs, there is visible deviation from the experimentally measured values. This can be attributed to the influence of the series resistance, which has an effect on the I-V characteristics of a PV module towards the V_{oc} region [50], which was assumed to be zero in the method proposed in this research. It however has no effect on the maximum power point as it can be shown by the results obtained in table 4.4.

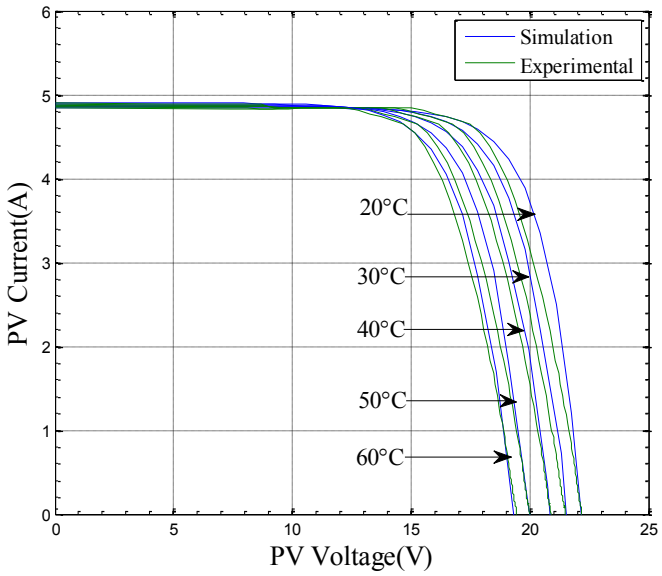

Figure 4.20 I-V Characteristic plot for SQ80 under varying Temperature for simulation and experimentally measured values

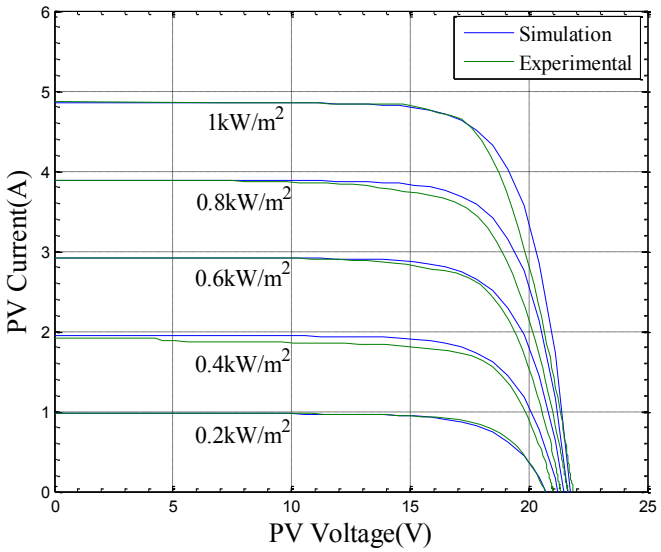

Figure 4.21 I-V Characteristic plot for SQ80 under varying Irradiance for simulation and experimentally measured values

4.6 Conclusion

In this chapter a new PV modelling method based on the simplified double-diode model is presented in this paper. The three different key operating points of a PV cell / module, that is the short circuit, open circuit and maximum power point operating conditions, are used to derive five equations which are used to estimate STC parameters for different PV modules. An algorithm is also proposed which is used to estimate the ideality factors of the two diodes by using only the datasheet parameters as the input. The algorithm was tested by estimating the ideality factors as well as the three currents, I_{o1}, I_{o2} and I_{ph} for five different PV modules. Values of maximum power calculated from the estimated parameters were compared with values obtained using results in [8] and [34] as well as the values from the datasheet. The results showed that the proposed method has accurate results.

A set of equations is used for calculating the reverse saturation currents I_{o1} and I_{o2} under varying irradiance and temperature. A correction factor that is dependent on G is introduced in the equations for calculating current, to cater for the effects of the change in V_{oc} due to change in irradiance. The estimated parameters have been used to plot the I-V characteristics of three different PV modules, the KC200GT, GEPV110 and SQ80 PV module and comparison made with extracts from datasheets for the respective PV modules. Validation of the proposed method is done by comparing simulation results with results obtained from experimental measurements on the SQ80 PV module, and it can be concluded that the results obtained using this method are accurate.

5 Conclusion and Future work

5.1 Conclusions

In this dissertation, a literature review was done on modelling of PV modules or cells. Two representations of a PV module were identified, the single-diode and the double-diode representation. The main aim of this study is to identify the most accurate PV modelling method based on the parameter estimation methods in combination with the different models. Different methods were identified in literature which were used to model PV modules using the single-diode representation. Two parameter estimation methods were identified and classified as method A and method B as well as five unique combinations of modelling equations which were classified as model 1, model 2, model 3, model 4 and model 5 and were used in the analysis. The objective was to identify a combination of parameter estimation method and the set of modelling equations which produced the most accurate representation of different PV modules of different types and ratings. Accuracy of the modelling methods was evaluated by comparing the results or graphs obtained from simulations with graphs extracted from manufacturer's datasheets for KC200GT PV module as well as comparison with experimentally measured values for the SQ80 PV module.

Parameter estimation method A which uses iteration technique to solve a system of equations was identified as the more accurate method based on the fact that it produced I-V characteristic plots which closely resemble the plots on the datasheet of the KC200GT PV module as well as the experimentally measured values for the SQ80 PV module. The combination of modelling equations classified as model 4 was also identified as the most accurate based on the I-V characteristic plots it generated. It can be concluded therefore that the combination of parameter estimation method A and model 4 equations produces the most accurate model for the single-diode representation of any PV module using PV module manufacture's datasheet parameters as inputs.

The double-diode representation of a PV module was also analysed and a new method was proposed which is an improvement on an existing model that is presented in [8], which has inaccuracies especially when non STC conditions are considered. The improved modelling method was verified to be accurate using datasheet information for different PV modules of different technologies and ratings as well as measured data for the SQ80 PV module as it produced results which have less error than the ones produced

by models used in [8] and [34]. This evaluation was based on accurately matching the three operating points, short circuit, open circuit and maximum power point on the I-V characteristic. It can be concluded based on the above analysis and discussions that a more accurate 'simplified double-diode' version of PV modelling method has been presented.

5.2 Future Work

Following the conclusion discussed in section 5.1, there are areas of improvement which future research can be directed towards as far as the PV modelling subject is concerned and are listed as follows:

- The effects of temperature and irradiance is currently only considered for two of the 5 estimated parameters, even though they are assumed not to change, it can be interesting to see further investigation of the results if the effects are taken into consideration for all the parameters, the effect on the other parameters is said to be minimal.
- In improving the double-diode model, one of the major challenges was the reverse saturation currents being positive. A review of the direction of current flow especially on the second diode to investigate a possibility that the current could flow in the opposite direction to the one currently used in the double-diode representation, due to physical or fabrication properties is required.
- Extend the double-diode model to include the series and shunt resistances without making assumptions which are in most cases invalid to try and reduce the complexity of the expressions.

References

[1] Carnegie Institution. "Solar could meet California energy demand three to five times over." *Science Daily*, para. 1-2, March 16, 2015, Available: http://www.sciencedaily.com/releases/2015/03/150316135152.htm

[2] P. Suskis, I. Galkin, "Enhanced photovoltaic panel model for MATLAB-simulink environment considering solar cell junction capacitance", *Industrial Electronics Society, IECON 2013 - 39th Annual Conference of the IEEE*, pp.1613-1618, 10-13 Nov. 2013.

[3] http://www.energy.gov.za/files/esources/renewables/r_solar.html

[4] N. Greve, "South Africa emerges as top renewable-energy investment destination", *Creamer Media's Engineering News*, para. 1-7, February 6, 2015, Available: http://www.engineeringnews.co.za/article/sa-top-renewable-energy-investment-destination-says-global-firm-2015-02-06

[5] S. Moodley, "Renewables' contribution to SA's power mix set to grow", *Creamer Media's Engineering News*, para. 1-9, June 13, 2014, Available: http://www.engineeringnews.co.za/article/renewables-to-contribute-42-to-national-energy-grid-by-2030-2014-06-13.

[6] M. C. DiPiazza, G. Vitale, "Photovoltaic source model" in *Photovoltaic sources: modelling and emulation*, Springer Science and Business Media, London; Springer-Verlag London, 2013, pp. 59.

[7] F. Attivissimo, A. Di Nisio, M. Savino, M. Spadavecchia, "Uncertainty Analysis in Photovoltaic Cell Parameter Estimation", *IEEE Transactions on Instrumentation and Measurement,* vol.61, pp.1334-1342, May 2012.

[8] B. C. Babu, S. Gurjar, "A Novel Simplified Two-Diode Model of Photovoltaic (PV) Module," *IEEE Journal of Photovoltaics,* vol.4, pp.1156-1161, July 2014

[9] A. J. Buhler, A. Krenzinger, "Method for photovoltaic parameter extraction according to a modified double-diode model", *Journal of Progress in photovoltaics: Research and applications,* vol. 21, pp.884-893, August 2013.

[10] E.I. Batzelis, I.A. Routsolias, S.A. Papathanassiou, "An Explicit PV String Model Based on the Lambert Function and Simplified MPP Expressions for Operation Under Partial Shading", *IEEE Transactions on Sustainable Energy,* vol.5, pp.301-312, Jan. 2014.

[11] F. Spertino, J. Sumaili, H. Andrei, G. Chicco, "PV Module Parameter Characterization From the Transient Charge of an External Capacitor" *IEEE Journal of Photovoltaics,* vol.3, no.4, pp.1325-1333, Oct. 2013.

[12] M. Ahmad, A. A. Talukder, M. A. Tanni, "Estimation of important parameters of photovoltaic modules from manufacturer's datasheet" 2012 *International Conference on Informatics, Electronics & Vision (ICIEV)*, pp.571-576, 18-19 May 2012.

[13] M. C. Di Piazza, M. Luna, G. Vitale, "Dynamic PV Model Parameter Identification by Least-Squares Regression", *IEEE Journal of Photovoltaics*, vol.3, no.2, pp.799-806, April 2013.

[14] D. S. H. Chan, J. C. H. Phang, "Analytical methods for the extraction of solar-cell single- and double-diode model parameters from I-V characteristics", *IEEE Transactions on Electron Devices*, vol.34, no.2, pp.286-293, Feb 1987.

[15] S. Moballegh, J. Jiang, "Modeling, Prediction, and Experimental Validations of Power Peaks of PV Arrays Under Partial Shading Conditions", *IEEE Transactions on Sustainable Energy*, vol.5, no.1, pp.293-300, Jan. 2014.

[16] S. M. Petcut, T. Dragomir, “Solar Cell Parameter Identification Using Generic Algorithms", Journal *of Control Engineering and Applied Informatics*, vol.12, No.1, pp.30-37, 2010.

[17] M. Wolf, G. T. Noel, R. J. Stirn, "Investigation of the double exponential in the current—Voltage characteristics of silicon solar cells," *IEEE Transactions on Electron Devices*, vol.24, pp.419-428, Apr 1977.

[18] G. H. Yordanov. O. M. Midtgard, T. O. Saetre, "Extracting parameters from semi-log plots of polycrystalline silicon PV modules outdoor I–V data: Double-exponential model revisited," in Proc. *2010 35th IEEE Photovoltaic Specialists Conference (PVSC)*, 20-25 June 2010, pp.2756-2761.

[19] H. Andrei, T. Ivanovici, G. Predusca, E. Diaconu, P. C. Andrei, "Curve fitting method for modeling and analysis of photovoltaic cells characteristics", 2012 *IEEE International Conference on Automation Quality and Testing Robotics (AQTR)*, pp.307-312, 24-27 May 2012.

[20] A. Chatterjee, A. Keyhani, D. Kapoor, "Identification of Photovoltaic Source Models", *IEEE Transactions on Energy Conversion*, vol.26, no.3, pp.883-889, Sept. 2011.

[21] Y. A. Mahmoud, X. Weidong, H. H. Zeineldin,"A Parameterization Approach for Enhancing PV Model Accuracy", *IEEE Transactions on Industrial Electronics*, vol.60, no.12, pp.5708-5716, Dec. 2013.

[22] S. A. Rahman, R. K. Varma, T. Vanderheide, "Generalised model of a photovoltaic panel," *Renewable Power Generation, IET*, vol.8, no.3, pp.217-229, April 2014.

[23] S. Jing Jun, L. Kay-Soon, "Optimizing photovoltaic model parameters for simulation", *2012 IEEE International Symposium on Industrial Electronics (ISIE)*, pp.1813-1818, 28-31 May 2012.

[24] H. A. B. Siddique, X. Ping, R. W. De Doncker, "Parameter extraction algorithm for one-diode model of PV panels based on datasheet values", *2013 International Conference on Clean Electrical Power (ICCEP)*, pp.7-13, 11-13 June 2013.

[25] Y. Mahmoud, W. Xiao, H. H. Zeineldin, "A Simple Approach to Modeling and Simulation of Photovoltaic Modules", *IEEE Transactions on Sustainable Energy*, vol.3, no.1, pp.185-186, Jan. 2012.

[26] M. A. de Blas, J. L. Torres, E. Prieto, A. García," Selecting a suitable model for characterizing photovoltaic devices", *Transactions on Renewable Energy*, vol.25, no.3, pp.371–380, Mar. 2002.

[27] D. Sera, R. Teodorescu, P. Rodriguez, "PV panel model based on datasheet values", *2007 IEEE International Symposium on Industrial Electronics (ISIE)*, pp.2392-2396, 4-7 Jun. 2007.

[28] S. Jing Jun, L. Kay-Soon, "Photovoltaic Model Identification Using Particle Swarm Optimization With Inverse Barrier Constraint", *IEEE Transactions on Power Electronics*, vol.27, no.9, pp.3975-3983, Sept. 2012.

[29] M. G. Villalva, J. R. Gazoli, E.R. Filho, "Comprehensive Approach to Modeling and Simulation of Photovoltaic Arrays", *IEEE Transactions on Power Electronics*, vol.24, no.5, pp.1198-1208, May 2009.

[30] H. Park, H. Kim, "PV cell modeling on single-diode equivalent circuit", *Industrial Electronics Society, IECON 2013 - 39th Annual Conference of the IEEE*, pp.1845-1849, 10-13 Nov. 2013.

[31] M. M. H. Islam, S. Z. Djokic, J. Desmet, B. Verhelst, "Measurement-based modelling and validation of PV systems", *2013 IEEE Grenoble PowerTech (POWERTECH)*, pp.1-6, 16-20 June 2013.

[32] S. A. Rahman, R. K. Varma, T. Vanderheide, "Generalised model of a photovoltaic panel," *Renewable Power Generation, IET*, vol.8, no.3, pp.217-229, April 2014.

[33] L. Sandrolini, M. Artioli, U. Reggiani, “Numerical method for the extraction of photovoltaic module double-diode model parameters through cluster analysis,” *Journal of Applied Energy*, vol.87, pp. 442–451, 2010

[34] M. Hejri, H. Mokhtari,M. R. Azizian, M. Ghandhari, L. Soder, "On the Parameter Extraction of a Five-Parameter Double-Diode Model of Photovoltaic Cells and Modules," *Journal of photovoltaics, IEEE*, vol.4, pp.915-923, May 2014.

[35] S. Islam, M. IqbaBaharChowdhury, " Simulation of two-diode model based PV solar cell/ array: A Simulink model Approach", *1st international conference on research in Science, Engineering and Management (IOCRSEM)*, pp.1-4, 27-29 March 2012.

[36] M. R. AlRashidi, K. M. El-Naggar, M. F. AlHajri “Parameters Estimation of Double-diode Solar Cell Model” , *International Journal of Electrical, Computer, Electronics and Communication Engineering*, vol.7, 2013.

[37] E. Q. B. Macabebe, E. E. van Dyk, “Parameter extraction from dark current–voltage characteristics of solar cells”, *South African Journal of Science,* vol.104, September/October 2008

[38] Z. Salam, K. Ishaque, H. Taheri, "An improved two-diode photovoltaic (PV) model for PV system," in Proc. *Joint international conference on Power Electronics, Drives and Energy Systems (PEDES) & 2010 Power India,* 20-23 Dec. 2010, pp.1-5.

[39] M. Wolf, G. T. Noel, R. J. Stirn, "Investigation of the double exponential in the current—Voltage characteristics of silicon solar cells," *IEEE Transactions on Electron Devices*, vol.24, pp.419-428, Apr 1977.

[40] S. Gupta, H. Tiwari, M. Fozdar, V. Chandna, "Development of a Two Diode Model for Photovoltaic Modules Suitable for Use in Simulation Studies," in Proc. *2012 Asia-Pacific Power and Energy Engineering Conference (APPEEC),* 27-29 March 2012, pp.1-4.

[41] P. Junsangsri, M. Lombardi, P. Fabrizio, "Double-diode modeling of time/temperature induced degradation of solar cells," in Proc. *2010 53rd IEEE International Midwest Symposium on Circuits and Systems (MWSCAS)*, 1-4 Aug. 2010, pp.1005-1008.

[42] B. Alsayid, “Modeling and Simulation of Photovoltaic Cell/Module/Array with Two-Diode Model,” *International Journal of Computer Technology and Electronics Engineering (IJCTEE),*vol.1, Jun 2012

[43] N. Femia, G. Petrone, G. Spagnuolo, M. Vitelli., “PV Modeling,” in Power Electronics and Control Techniques for Maximum Energy Harvesting in Photovoltaic Systems. Boca Raton: CRC Press, 2013. pp. 11-15.

[44] Shell Solar, “Photovoltaic Solar Module”, SQ80 Datasheet.

[45] Kyocera KC200GT datasheet. Available: http://www.kyocerasolar.com/assets/001/5195.pdf

[46] BP solar MSX-60. (1997). [Online]. Available: *www.solarelectricsupply.com/media/custom/upload/Solarex-MSX64.pdf.*

[47] Rensola JC260S. (1998). [Online]. Available: www.civicsolar.com/ sites/default/files/documents/156-series-mono-245–260w-71327.pdf

[48] GEPV-110,110 watt photovoltaic module. [Online]. Available: http:// www.powerupco.com/panels/ge/GEPV-110 Product Data Sheet.pdf

[49] Kaneka Hybrid PV, Thin film hybrid solar panel, U-EA Type datasheet. [Online]. Available: http://www.kaneka-solar.com/product/thin-film/pdf/U-EA.pdf.

[50] W. D. Soto, S. A. Klein, and W. A. Beckman, “Improvement and validation of a model for photovoltaic array performance,” *Sol. Energy*, vol.80, pp. 78–88, Aug. 2006.

Appendix A Matlab function code for parameter estimation using Method A

```
function [Io, Iph, Rs, Rsh, A] = EST_A(Isc, Voc, Vmp, Imp, Ns)
%This function takes STC datasheet parameters for any particular PV module
%and returns the STC parameters Rs, Rsh, Ion, Iphn and A. The method used
%is method A as indicated.

q=1.602e-19;    %assign electron charge value
K=1.38e-23;     %assign boltzman's constant

kmax=22;        %set maximum number of iterations to 22
x1=zeros(1,100);%assign array for Rs
x2=zeros(1,100);%assign array for Rsh
x3=zeros(1,100);%assign array for Vt
k=1;
x1(:,k)=0;      %set initial value of Rs to zero
x2(:,k)=1000;   %set initial value of Rsh to 1000
x3(:,k)=(Imp*x1(:,k)+Vmp-Voc)/(Ns*log((((Isc-Imp)*(x1(:,k)+x2(:,k)))-Vmp)/((Isc*(x1(:,k)+x2(:,k)))-Voc))); %calculate initial value of
                                                                                                            Vt from (3.20)

% For 22 iterations, calculate new values for Rsh from (3.26), Rs from (3.23) and Vt from (3.20)
while k<=kmax
    x2(:,k+1)=(Ns*x3(:,k)*x1(:,k)+Ns*x3(:,k)*x2(:,k)+(x1(:,k)*exp((Isc*x1(:,k)-Voc)/(Ns*x3(:,k)))*(Isc*x1(:,k)+Isc*x2(:,k)-Voc)))/
              (Ns*x3(:,k)+(exp((-Voc)/(Ns*x3(:,k)))*(Isc*x1(:,k)+Isc*x2(:,k)-Voc)));

    x1(:,k+1)=(Voc-Vmp+Ns*x3(:,k)*log(Ns*x3(:,k)*(Imp*x1(:,k)+Imp*x2(:,k)-Vmp)/(Isc*Vmp*x3(:,k)+Isc*Vmp*x2(:,k)+Imp*Voc*x1(:,k)-
              Isc*Imp*(x1(:,k))^2-Imp*Isc*x2(:,k)*x1(:,k)-Voc*Vmp)))/(Imp);

    x3(:,k+1)=(Imp*x1(:,k+1)+Vmp-Voc)/(Ns*log(((Isc-Imp)*(x1(:,k+1)+x2(:,k+1))-Vmp)/(Isc*(x1(:,k+1)+x2(:,k+1))-Voc)));

    k=k+1;
end


Rs=x1(:,k);             %current value of x1 is the solution for Rs
Vtn=x3(:,k);            %current value of x3 is the solution for Vt
A=q*(x3(:,k))/(K*298);  %calculate A from current value of Vt
Rsh=x2(:,k);            %current value of x2 is the solution for Rsh
Ion=(Isc*Rsh+Isc*Rs-Voc)/(Rsh*exp(Voc/(Ns*Vtn))); %calculate Ion from (3.14)
Iphn=Ion*(exp(Voc/(Ns*Vtn))-1)+(Voc/Rsh);       %calculate Iphn from (3.3)


end
```

Appendix B Matlab function code for parameter estimation using Method B

```
function [A, Rs, Ion, Iphn, Rsh] = EST_B(Isc, Voc, Vmp, Imp, Ki, Kv, Ns)
%This function takes STC datasheet parameters for any particular PV module
%and returns STC parameters Rs, Rsh, Iphn, Ion and A. The method used is
%method B as indicated

q=1.602e-19;    %assign electron charge
K=1.38e-23;     %assign boltzman's constant
Ego=1.166;      %assign fitting parameter
B=636;          %assign fitting parameter
M=4.7e-4;       %assign fitting parameter

%These are STC paraeters which are used for the estimation of the five STC
%unknown parameters

VTn=K*298/q;    %calculate Vt at T=298K
Pmax=Vmp*Imp;   %assign value for maximum power
Egn=Ego-((M*298^2)/(298+B)); %calculate band gap energy using (3.36) for T=298K
Iphn=Isc; %set initial value of Iphn to Isc, corresponding to Rs=0 in (3.27)
A=(Kv-(Voc/298))/(Ns*VTn*((Ki/Iphn)-(3/298)-(q*Egn/(K*298^2)))); %calculate A from (3.35)

P=zeros(1,10*Voc+1);
I=zeros(1,10*Voc+1);

%Initialize Rs, Rsh and Io
Rs=0;
Rsh=(Vmp/(Isc-Imp))-((Voc-Vmp)/Imp);   %calculate Rsh from (3.40)
Ion=(Isc*Rs+Isc*Rsh-Voc)/(Rsh*exp((Voc)/(Ns*Vtn))); %calculate Ion from (3.14)

errorPmax=1; %initialize constant


while errorPmax > 0.01
     Iphn=(1+(Rs/Rsh))*Isc; %calculate Iphn from (3.27)
     V=(0:0.1:Voc);
     I=Iphn-((V+I*Rs)/Rsh)-Ion*(exp((V+I*Rs)/(Ns*A*Vtn))-1);

     for k=1:(10*Voc+1)
     P(1,k)=V(1,k)*I(1,k);
     end

     errorPmax=abs(Pmax-max(P));

     if errorPmax > 0.01
        Rs=Rs+0.01; %increment Rs
        Rsh=(Vmp*(Vmp+Imp*Rs))/(Vmp*Iphn+Vmp*Ion-Pmax-Vmp*Ion*exp((Vmp+Imp*Rs)*q/(Ns*An*K*298))); %calculate Rsh from (3.40)
        Ion=(Isc*Rs+Isc*Rsh-Voc)/(Rsh*exp((Voc)/(Ns*Vtn))); %calculate Ion from (3.14)
     end

end


end
```

Appendix C Matlab function code for parameter estimation for double-diode model

```
function [Iph, Io1, Io2, A1, A2] = TwoDiode(Vmp, Voc, Isc, Imp, Ns)
%This function is used to estimate the five unknown STC parameters for the
%simplified double-diode model. It takes STC datasheet parameters as inputs.
% It uses A1=1 and first finds the minimum value of A2 for which both
% reverse saturation currents are positive. The next level is to check if
% the maximum power decreases or increases as the value of A2 is increased.
% If maximum power decreases, A2 is increased until a minimum value of
% maximum power is reached or a value almost equal to the STC maximum power
% value.

K=1.38e-23;     %assign boltzma's constant
T=298;          %set T=298K for STC conditions
q=1.6e-19;      %assign electron charge
VT=Ns*K*T/q;    %calculate the thermal voltage ast STC

A1=1;   %initialize ideality factor A1
A2=1;   %initialize ideality factor A2

%set arbitrary values for Io1 and Io2 to initiate the while loop
Io1=-1;
Io2=-1;
%Find the minimum value of A2 for which both reverse saturation currents
%are positive. Iph is calculated from (4.2), Io1 from (4.11) and Io2 from
%(4.10)
while Io1 < 0 || Io2 < 0
    A2=A2+0.01;
    Io2=((Imp-Isc)*exp(Voc/(A1*VT))+Isc*exp(Vmp/(A1*VT)))/(exp(Voc/(A2*VT))*exp(Vmp/(A1*VT))-exp(Vmp/(A2*VT))*exp(Voc/(A1*VT)));
    Io1=Isc*exp(-(Voc/(A1*VT)))-Io2*exp(Voc/(A2*VT))/exp(Voc/(A1*VT));
    Iph=Isc;
end
%Find maximum power value at A2(min) and assign it as Pmax_old
I=zeros(1, 10*Voc+1);
P=zeros(1, 10*Voc+1);
     V=(0:0.1:Voc);
     I=Iph-Io1*(exp(V/(A1*VT))-1)-Io2*(exp(V/(A2*VT))-1);
     for k=1: 10*Voc+1
     P(1,k)=V(1,k)*I(1,k);
     end
Pmax_old=max(P);

%Increment A2 and find a new value of maximum power
    A2=A2+0.01;
    Io2=((Imp-Isc)*exp(Voc/(A1*VT))+Isc*exp(Vmp/(A1*VT)))/(exp(Voc/(A2*VT))*exp(Vmp/(A1*VT))-exp(Vmp/(A2*VT))*exp(Voc/(A1*VT)));
    Io1=Isc*exp(-(Voc/(A1*VT)))-Io2*exp(Voc/(A2*VT))/exp(Voc/(A1*VT));
    Iph=Isc;

    I=zeros(1, 10*Voc+1);
    P=zeros(1, 10*Voc+1);

    V=(0:0.1:Voc);
    I=Iph-Io1*(exp(V/(A1*VT))-1)-Io2*(exp(V/(A2*VT))-1);
    for k=1: 10*Voc+1
      P(1,k)=V(1,k)*I(1,k);
    end
Pmax_new=max(P);
%If the new power value is less than the old value then enter loop and
%increment the value of A2 until the maxumum power values stop decreasing
%or are very close to the datasheet STC value of maximum power
error=1;
while Pmax_old > Pmax_new && error > 0.01

    A2=A2+0.01;
    Io2=((Imp-Isc)*exp(Voc/(A1*VT))+Isc*exp(Vmp/(A1*VT)))/(exp(Voc/(A2*VT))*exp(Vmp/(A1*VT))-exp(Vmp/(A2*VT))*exp(Voc/(A1*VT)));
    Io1=Isc*exp(-(Voc/(A1*VT)))-Io2*exp(Voc/(A2*VT))/exp(Voc/(A1*VT));
    Iph=Isc;

    I=zeros(1, 10*Voc+1);
    P=zeros(1, 10*Voc+1);

    V=(0:0.1:Voc);
    I=Iph-Io1*(exp(V/(A1*VT))-1)-Io2*(exp(V/(A2*VT))-1);
    for k=1: 10*Voc+1
     P(1,k)=V(1,k)*I(1,k);
    end
    Pmax_old=Pmax_new;
    Pmax_new=max(P);
end
%Assign final values to be returned by function
A2=A2-0.01;
Io2=((Imp-Isc)*exp(Voc/(A1*VT))+Isc*exp(Vmp/(A1*VT)))/(exp(Voc/(A2*VT))*exp(Vmp/(A1*VT))-exp(Vmp/(A2*VT))*exp(Voc/(A1*VT)));
Io1=Isc*exp(-(Voc/(A1*VT)))-Io2*exp(Voc/(A2*VT))/exp(Voc/(A1*VT));
Iph=Isc;

end
```

Appendix D Experimental measurements for SQ80 PV Module

Table D.1 Data measured under varying temperature at 1kW/m^2

Temp 20 °C		Temp 30 °C		Temp 40 °C		Temp 50 °C		Temp 60 °C	
V	I	V	I	V	I	V	I	V	I
0	4.839	0	4.851	0	4.872	0	4.89	0	4.9
7.34	4.829	6.64	4.841	6.04	4.862	5.14	4.88	4.59	4.89
7.77	4.829	7.07	4.841	6.47	4.862	5.57	4.88	5.02	4.89
8.298	4.828	7.598	4.84	6.998	4.861	6.098	4.879	5.548	4.889
8.819	4.824	8.119	4.836	7.519	4.857	6.619	4.875	6.069	4.885
9.335	4.823	8.635	4.835	8.035	4.856	7.135	4.874	6.585	4.884
9.862	4.823	9.162	4.835	8.562	4.856	7.662	4.874	7.112	4.884
10.39	4.847	9.687	4.847	9.087	4.854	8.187	4.872	7.637	4.882
10.91	4.847	10.21	4.847	9.611	4.847	8.711	4.872	8.161	4.882
11.44	4.847	10.74	4.847	10.14	4.847	9.238	4.847	8.688	4.882
11.97	4.844	11.27	4.844	10.67	4.844	9.769	4.844	9.219	4.844
12.5	4.843	11.8	4.843	11.2	4.843	10.3	4.843	9.745	4.843
13.01	4.843	12.31	4.843	11.71	4.843	10.81	4.843	10.26	4.843
13.53	4.843	12.83	4.843	12.23	4.843	11.33	4.843	10.78	4.843
14.03	4.843	13.33	4.843	12.73	4.843	11.83	4.843	11.28	4.843
14.53	4.843	13.83	4.843	13.23	4.843	12.33	4.843	11.78	4.843
15.02	4.843	14.32	4.843	13.72	4.843	12.82	4.843	12.27	4.843
15.52	4.807	14.82	4.807	14.22	4.807	13.32	4.807	12.77	4.807
16.02	4.769	15.32	4.769	14.72	4.769	13.82	4.769	13.27	4.769
16.5	4.734	15.8	4.734	15.2	4.734	14.3	4.734	13.75	4.734
16.99	4.7	16.29	4.7	15.69	4.7	14.79	4.7	14.24	4.7
17.46	4.649	16.76	4.649	16.16	4.649	15.26	4.649	14.71	4.649
17.91	4.544	17.21	4.544	16.61	4.544	15.71	4.544	15.16	4.544
18.33	4.385	17.63	4.385	17.03	4.385	16.13	4.385	15.58	4.385
18.71	4.189	18.01	4.189	17.41	4.189	16.51	4.189	15.96	4.189
19.06	3.973	18.36	3.973	17.76	3.973	16.86	3.973	16.31	3.973
19.37	3.743	18.67	3.743	18.07	3.743	17.17	3.743	16.62	3.743
19.66	3.503	18.96	3.503	18.36	3.503	17.46	3.503	16.91	3.503
19.91	3.264	19.21	3.264	18.61	3.264	17.71	3.264	17.16	3.264
20.14	3.03	19.44	3.03	18.84	3.03	17.94	3.03	17.39	3.03
20.35	2.802	19.65	2.802	19.05	2.802	18.15	2.802	17.6	2.802
20.54	2.582	19.84	2.582	19.24	2.582	18.34	2.582	17.79	2.582
20.69	2.374	19.99	2.374	19.39	2.374	18.49	2.374	17.94	2.374
20.84	2.179	20.14	2.179	19.54	2.179	18.64	2.179	18.09	2.179
20.97	2.003	20.27	2.003	19.67	2.003	18.77	2.003	18.22	2.003
21.1	1.831	20.4	1.831	19.8	1.831	18.9	1.831	18.35	1.831
21.21	1.681	20.51	1.681	19.91	1.681	19.01	1.681	18.46	1.681
21.3	1.54	20.6	1.54	20	1.54	19.1	1.54	18.55	1.54
21.39	1.411	20.69	1.411	20.09	1.411	19.19	1.411	18.64	1.411
21.46	1.294	20.76	1.294	20.16	1.294	19.26	1.294	18.71	1.294

21.53	1.186	20.83	1.186	20.23	1.186	19.33	1.186	18.78	1.186
21.59	1.088	20.89	1.088	20.29	1.088	19.39	1.088	18.84	1.088
21.64	0.995	20.94	0.995	20.34	0.995	19.44	0.995	18.89	0.995
21.7	0.914	21	0.914	20.4	0.914	19.5	0.914	18.95	0.914
21.74	0.845	21.04	0.845	20.44	0.845	19.54	0.845	18.99	0.845
21.78	0.78	21.08	0.78	20.48	0.78	19.58	0.78	19.03	0.78
21.81	0.714	21.11	0.714	20.51	0.714	19.61	0.714	19.06	0.714
21.84	0.657	21.14	0.657	20.54	0.657	19.64	0.657	19.09	0.657
21.88	0.61	21.18	0.61	20.58	0.61	19.68	0.61	19.13	0.61
21.89	0.565	21.19	0.565	20.59	0.565	19.69	0.565	19.14	0.565
21.91	0.521	21.21	0.521	20.61	0.521	19.71	0.521	19.16	0.521
21.93	0.478	21.23	0.478	20.63	0.478	19.73	0.478	19.18	0.478
21.95	0.443	21.25	0.443	20.65	0.443	19.75	0.443	19.2	0.443
21.96	0.414	21.26	0.414	20.66	0.414	19.76	0.414	19.21	0.414
21.98	0.388	21.28	0.388	20.68	0.388	19.78	0.388	19.23	0.388
21.99	0.365	21.29	0.365	20.69	0.365	19.79	0.365	19.24	0.365
22.01	0.338	21.31	0.338	20.71	0.338	19.81	0.338	19.26	0.338
22.02	0.315	21.32	0.315	20.72	0.315	19.82	0.315	19.27	0.315
22.03	0.295	21.33	0.295	20.73	0.295	19.83	0.295	19.28	0.295
22.04	0.275	21.34	0.275	20.74	0.275	19.84	0.275	19.29	0.275
22.05	0.262	21.35	0.262	20.75	0.262	19.85	0.262	19.3	0.262
22.05	0.245	21.35	0.245	20.75	0.245	19.85	0.245	19.3	0.245
22.05	0.23	21.35	0.23	20.75	0.23	19.85	0.23	19.3	0.23
22.07	0.216	21.37	0.216	20.77	0.216	19.87	0.216	19.32	0.216
22.07	0.204	21.37	0.204	20.77	0.204	19.87	0.204	19.32	0.204
22.07	0.195	21.37	0.195	20.77	0.195	19.87	0.195	19.32	0.195
22.08	0.182	21.38	0.182	20.78	0.182	19.88	0.182	19.33	0.182
22.09	0.17	21.39	0.17	20.79	0.17	19.89	0.17	19.34	0.17
22.09	0.162	21.39	0.162	20.79	0.162	19.89	0.162	19.34	0.162
22.1	0.155	21.4	0.155	20.8	0.155	19.9	0.155	19.35	0.155
22.12	0.148	21.42	0.148	20.82	0.148	19.92	0.148	19.37	0.148
22.12	0.141	21.42	0.141	20.82	0.141	19.92	0.141	19.37	0.141
22.12	0.135	21.42	0.135	20.82	0.135	19.92	0.135	19.37	0.135
22.13	0.128	21.43	0.128	20.83	0.128	19.93	0.128	19.38	0.128
22.14	0.123	21.44	0.123	20.84	0.123	19.94	0.123	19.39	0.123
22.13	0.12	21.43	0.12	20.83	0.12	19.93	0.12	19.38	0.12
22.13	0.112	21.43	0.112	20.83	0.112	19.93	0.112	19.38	0.112
22.14	0.105	21.44	0.105	20.84	0.105	19.94	0.105	19.39	0.105
22.15	0.105	21.45	0.105	20.85	0.105	19.95	0.105	19.4	0.105
22.14	0.1	21.44	0.1	20.84	0.1	19.94	0.1	19.39	0.1
22.15	0.095	21.45	0.095	20.85	0.095	19.95	0.095	19.4	0.095
22.17	0.092	21.47	0.092	20.87	0.092	19.97	0.092	19.42	0.092
22.16	0.088	21.46	0.088	20.86	0.088	19.96	0.088	19.41	0.088
22.16	0.087	21.46	0.087	20.86	0.087	19.96	0.087	19.41	0.087

22.17	0.085	21.47	0.085	20.87	0.085	19.97	0.085	19.42	0.085
22.17	0.08	21.47	0.08	20.87	0.08	19.97	0.08	19.42	0.08
22.16	0.075	21.46	0.075	20.86	0.075	19.96	0.075	19.41	0.075
22.17	0.075	21.47	0.075	20.87	0.075	19.97	0.075	19.42	0.075
22.18	0.076	21.48	0.076	20.88	0.076	19.98	0.076	19.43	0.076
22.18	0.069	21.48	0.069	20.88	0.069	19.98	0.069	19.43	0.069
22.18	0.065	21.48	0.065	20.88	0.065	19.98	0.065	19.43	0.065
22.18	0.061	21.48	0.061	20.88	0.061	19.98	0.061	19.43	0.061
22.17	0.062	21.47	0.062	20.87	0.062	19.97	0.062	19.42	0.062
22.18	0.064	21.48	0.064	20.88	0.064	19.98	0.064	19.43	0.064
22.18	0.061	21.48	0.061	20.88	0.061	19.98	0.061	19.43	0.061
22.17	0.06	21.47	0.06	20.87	0.06	19.97	0.06	19.42	0.06
22.18	0.06	21.48	0.06	20.88	0.06	19.98	0.06	19.43	0.06
22.17	0.06	21.47	0.06	20.87	0.06	19.97	0.06	19.42	0.06
22.17	0.058	21.47	0.058	20.87	0.058	19.97	0.058	19.42	0.058
22.17	0.041	21.47	0.041	20.87	0.041	19.97	0.041	19.42	0.041
22.2	0	21.5	0	20.9	0	20	0	19.45	0

Table D.2 Data measured under varying irradiance at 25 °C

Irradiance 1kW/m²		Irradiance 0.8 kW/m²		Irradiance 0.6 kW/m²		Irradiance 0.4 kW/m²		Irradiance 0.2 kW/m²	
V	I	V	I	V	I	V	I	V	I
0	4.865	0	3.881	0	2.913	0	1.908	0	0.97
7.02	4.855	5.93	3.881	4.69	2.913	4.24	1.908	4.67	0.97
7.45	4.855	6.35	3.877	5.06	2.919	4.553	1.88	4.98	0.979
7.978	4.853	6.9	3.877	5.61	2.919	5.066	1.875	5.48	0.98
8.499	4.85	7.46	3.877	6.19	2.92	5.629	1.873	6.01	0.981
9.015	4.849	8.04	3.873	6.77	2.919	6.199	1.869	6.55	0.981
9.542	4.849	8.61	3.869	7.35	2.917	6.76	1.866	7.07	0.979
10.07	4.847	9.18	3.864	7.94	2.913	7.324	1.868	7.6	0.978
10.59	4.847	9.76	3.862	8.52	2.912	7.89	1.868	8.15	0.977
11.12	4.847	10.3	3.857	9.11	2.911	8.436	1.863	8.69	0.976
11.65	4.844	10.9	3.852	9.69	2.909	8.998	1.86	9.23	0.975
12.18	4.843	11.5	3.845	10.3	2.908	9.552	1.861	9.77	0.975
12.69	4.843	12	3.839	10.8	2.906	10.1	1.857	10.3	0.972
13.21	4.843	12.6	3.829	11.4	2.902	10.65	1.856	10.9	0.97
13.71	4.843	13.1	3.813	12	2.894	11.21	1.855	11.4	0.967
14.21	4.843	13.7	3.794	12.6	2.888	11.75	1.852	11.9	0.962
14.7	4.843	14.2	3.771	13.2	2.878	12.29	1.846	12.4	0.961
15.2	4.807	14.8	3.748	13.7	2.864	12.85	1.841	12.9	0.96
15.7	4.769	15.3	3.723	14.3	2.849	13.39	1.838	13.5	0.958
16.18	4.734	15.8	3.691	14.8	2.829	13.94	1.833	14	0.953
16.67	4.7	16.4	3.664	15.4	2.805	14.49	1.823	14.5	0.949
17.14	4.649	16.9	3.622	15.9	2.78	15.02	1.81	15	0.942
17.59	4.544	17.4	3.546	16.4	2.758	15.55	1.796	15.5	0.933
18.01	4.385	17.8	3.434	17	2.729	16.09	1.778	16.1	0.923
18.39	4.189	18.3	3.287	17.5	2.671	16.6	1.761	16.6	0.91
18.74	3.973	18.7	3.111	18	2.58	17.1	1.734	17.1	0.893
19.05	3.743	19	2.917	18.4	2.455	17.59	1.692	17.5	0.869
19.34	3.503	19.3	2.709	18.8	2.301	18.04	1.631	18	0.835
19.59	3.264	19.6	2.497	19.2	2.127	18.46	1.548	18.4	0.787
19.82	3.03	19.9	2.287	19.5	1.944	18.86	1.442	18.8	0.726
20.03	2.802	20.1	2.083	19.7	1.755	19.2	1.323	19.2	0.651
20.22	2.582	20.3	1.887	20	1.57	19.5	1.192	19.5	0.564
20.37	2.374	20.4	1.704	20.2	1.397	19.76	1.056	19.7	0.475
20.52	2.179	20.6	1.536	20.3	1.234	19.97	0.927	20	0.384
20.65	2.003	20.7	1.382	20.5	1.087	20.14	0.807	20.2	0.297
20.78	1.831	20.8	1.24	20.6	0.952	20.3	0.695	20.3	0.219
20.89	1.681	20.9	1.113	20.7	0.834	20.41	0.599	20.5	0.15
20.98	1.54	21	0.999	20.8	0.734	20.53	0.517	20.6	0.088
21.07	1.411	21.1	0.9	20.9	0.647	20.62	0.443	20.7	0.036
21.14	1.294	21.1	0.811	20.9	0.572	20.68	0.382	20.7	0
21.21	1.186	21.2	0.733	21	0.506	20.74	0.33		

21.27	1.088	21.2	0.661	21	0.445	20.78	0.285		
21.32	0.995	21.3	0.598	21.1	0.395	20.81	0.247		
21.38	0.914	21.3	0.54	21.1	0.352	20.84	0.214		
21.42	0.845	21.3	0.489	21.1	0.315	20.86	0.19		
21.46	0.78	21.4	0.445	21.2	0.281	20.87	0.168		
21.49	0.714	21.4	0.404	21.2	0.252	20.9	0.147		
21.52	0.657	21.4	0.368	21.2	0.228	20.92	0.133		
21.56	0.61	21.4	0.338	21.2	0.208	20.93	0.118		
21.57	0.565	21.5	0.31	21.2	0.188	20.94	0.105		
21.59	0.521	21.5	0.286	21.2	0.171	20.96	0.095		
21.61	0.478	21.5	0.263	21.2	0.156	20.96	0.086		
21.63	0.443	21.5	0.242	21.2	0.143	20.97	0.081		
21.64	0.414	21.5	0.224	21.2	0.131	20.97	0.076		
21.66	0.388	21.5	0.209	21.3	0.121	20.98	0.07		
21.67	0.365	21.5	0.193	21.3	0.112	20.98	0.064		
21.69	0.338	21.5	0.177	21.3	0.104	20.99	0.06		
21.7	0.315	21.5	0.164	21.3	0.099	21	0.054		
21.71	0.295	21.5	0.155	21.3	0.094	20.99	0.052		
21.72	0.275	21.6	0.144	21.3	0.087	21	0.049		
21.73	0.262	21.6	0.137	21.3	0.081	20.99	0.046		
21.73	0.245	21.6	0.129	21.3	0.08	21	0.044		
21.73	0.23	21.6	0.12	21.3	0.075	20.99	0.044		
21.75	0.216	21.6	0.113	21.3	0.07	20.99	0.04		
21.75	0.204	21.6	0.11	21.3	0.067	21	0.037		
21.75	0.195	21.6	0.105	21.3	0.063	21.01	0.037		
21.76	0.182	21.6	0.101	21.3	0.06	21.02	0.037		
21.77	0.17	21.6	0.096	21.3	0.058	21.01	0.032		
21.77	0.162	21.6	0.089	21.3	0.056	21.01	0.033		
21.78	0.155	21.6	0.085	21.3	0.053	21.02	0.032		
21.8	0.148	21.6	0.082	21.3	0.052	21.02	0.031		
21.8	0.141	21.6	0.078	21.3	0.049	21.02	0.031		
21.8	0.135	21.6	0.075	21.3	0.047	21.02	0.029		
21.81	0.128	21.6	0.072	21.3	0.045	21.02	0.029		
21.82	0.123	21.6	0.069	21.3	0.043	21.02	0.029		
21.81	0.12	21.6	0.066	21.3	0.041	21.02	0.028		
21.81	0.112	21.6	0.065	21.3	0.041	21	0.029		
21.82	0.105	21.6	0.062	21.3	0.037	21	0.029		
21.83	0.105	21.6	0.06	21.3	0.037	21.01	0.027		
21.82	0.1	21.6	0.06	21.3	0.036	21.01	0.027		
21.83	0.095	21.6	0.059	21.3	0.034	21.01	0.027		
21.85	0.092	21.6	0.054	21.3	0.034	21.02	0.026		
21.84	0.088	21.6	0.054	21.3	0.036	21.03	0.024		
21.84	0.087	21.6	0.054	21.3	0.035	21.04	0.023		
21.85	0.085	21.6	0.05	21.3	0.034	21.04	0.021		

21.85	0.08	21.6	0.05	21.4	0.033	21.04	0.021		
21.84	0.075	21.6	0.05	21.3	0.032	21.03	0.022		
21.85	0.075	21.6	0.047	21.3	0.032	21.03	0.021		
21.86	0.076	21.6	0.045	21.3	0.035	21.02	0.024		
21.86	0.069	21.6	0.044	21.3	0.035	21.03	0.025		
21.86	0.065	21.6	0.045	21.3	0.034	21.03	0.024		
21.86	0.061	21.6	0.042	21.3	0.033	21.02	0.023		
21.85	0.062	21.6	0.04	21.3	0.033	21.01	0.021		
21.86	0.064	21.6	0.041	21.3	0.032	21.01	0.02		
21.86	0.061	21.6	0.041	21.3	0.03	21	0.019		
21.85	0.06	21.6	0.038	21.3	0.027	21.02	0.018		
21.86	0.06	21.6	0.038	21.3	0.025	21.03	0.02		
21.85	0.06	21.6	0.038	21.3	0.027	21.02	0.021		
21.85	0.058	21.6	0.039	21.3	0.03	21.03	0.02		
21.85	0	21.6	0.03	21.3	0.024	21.03	0.017		
		21.6	0	21.4	0	21.03	0		

Appendix E Assessment of Ethics in research

EBE Faculty: Assessment of Ethics in Research Projects (Rev2)

Any person planning to undertake research in the Faculty of Engineering and the Built Environment at the University of Cape Town is required to complete this form before collecting or analysing data. When completed it should be submitted to the supervisor (where applicable) and from there to the Head of Department. If any of the questions below have been answered YES, and the applicant is NOT a fourth year student, the Head should forward this form for approval by the Faculty EIR committee: submit to Ms Zulpha Geyer (Zulpha.Geyer@uct.ac.za; Chem Eng Building, Ph 021 650 4791). **NB: A copy of this signed form must be included with the thesis/dissertation/report when it is submitted for examination**

This form must only be completed once the most recent revision EBE EiR Handbook has been read.

Name of Principal Researcher/Student: **Samkeliso H. Shongwe** Department: **Electrical Engineering**

Preferred email address of the applicant: **shongwe.samkeliso@gmail.com**

If a Student: Degree: **MSc Electrical Engineering** Supervisor: **Dr. Moin Hanif**

If a Research Contract indicate source of funding/sponsorship: **N/A**

Research Project Title: **Analysis of Single-Diode and Improvement of Double-diode Photovoltaic source modelling methods and Techniques**

Overview of ethics issues in your research project:

Question 1: Is there a possibility that your research could cause harm to a third party (i.e. a person not involved in your project)?	YES	✓ NO
Question 2: Is your research making use of human subjects as sources of data? If your answer is YES, please complete Addendum 2.	YES	✓ NO
Question 3: Does your research involve the participation of or provision of services to communities? If your answer is YES, please complete Addendum 3.	YES	✓ NO
Question 4: If your research is sponsored, is there any potential for conflicts of interest? If your answer is YES, please complete Addendum 4.	YES	✓ NO

If you have answered YES to any of the above questions, please append a copy of your research proposal, as well as any interview schedules or questionnaires (Addendum 1) and please complete further addenda as appropriate. Ensure that you refer to the EiR Handbook to assist you in completing the documentation requirements for this form.

I hereby undertake to carry out my research in such a way that

- there is no apparent legal objection to the nature or the method of research; and
- the research will not compromise staff or students or the other responsibilities of the University;
- the stated objective will be achieved, and the findings will have a high degree of validity;
- limitations and alternative interpretations will be considered;
- the findings could be subject to peer review and publicly available; and
- I will comply with the conventions of copyright and avoid any practice that would constitute plagiarism.

Signed by:

	Full name and signature	Date
Principal Researcher/Student:	Samkeliso Shongwe	7 May 2015

This application is approved by:

Supervisor (if applicable):	Dr. Moin Hanif	07/05/15
HOD (or delegated nominee): *Final authority for all assessments with NO to all questions and for all undergraduate research.*	F BOSE	15/5/15
Chair : Faculty EIR Committee For applicants other than undergraduate students who have answered YES to any of the above questions.		